Title: Bryophyte stable isotope composition, diversity and biomass define tropical montane cloud forest extent

Aline B. Horwath[1,2]*, Jessica Royles[1]*, Richard Tito[3,4], José A. Gudiño[5], Noris Salazar Allen[5], William Farfan-Rios[3,6], Joshua M. Rapp[6,7], Miles R. Silman[6], Yadvinder Malhi[8], Varun Swamy[9], Jean Paul Latorre Farfan[3, 10], Howard Griffiths[1§]

* Authors contributed equally to this work.

§ Corresponding author: Howard Griffiths, hg230@cam.ac.uk, tel: +44 (0)1223 333946

Affiliations:

[1]Department of Plant Sciences, University of Cambridge, Downing Street, Cambridge CB2 3EA, UK

[2]Biological and Environmental Sciences, Faculty of Natural Sciences, University of Stirling, Stirling FK9 4LA, UK

[3]Herbario Vargas (CUZ), Universidad Nacional de San Antonio Abad del Cusco, Cusco, Peru

[4]Instituto de Biologia, Universidade Federal de Uberlândia, Uberlândia, MG, Brazil

[5]Smithsonian Tropical Research Institute, P.O. Box 0843-03092, Balboa, Ancon, Panama, Republic of Panama

[6]Department of Biology, Wake Forest University, Winston-Salem, North Carolina 27106, USA

[7]Harvard Forest, Harvard University, 324 North Main St., Petersham, MA 01366, USA

[8]Environmental Change Institute, School of Geography and the Environment, University of Oxford, Oxford, UK

[9]San Diego Zoo Institute for Conservation Research, 15600 San Pasqual Valley Road Escondido, CA 92027, USA

[10]Aarhus University, Aarhus, Denmark

Keywords: Amazonia, climate change, liverworts, Peruvian Andes, tropical montane cloud forest, $\delta^{13}C$

Abstract

Liverworts and mosses are a major component of the epiphyte flora of tropical montane forest ecosystems. Canopy access was used to analyse the distribution and vertical stratification of bryophyte epiphytes within tree crowns at nine forest sites across a 3400 m elevational gradient in Peru, from the Amazonian basin to the high Andes. The stable isotope compositions of bryophyte organic material ($^{13}C/^{12}C$ and $^{18}O/^{16}O$) are associated with surface water diffusive limitations and, along with C/N content, provide a generic index for the extent of cloud immersion. From lowland to cloud forest $\delta^{13}C$ increased from -33‰ to -27‰, whilst $\delta^{18}O$ increased from 16.3 to 18.0‰. Epiphytic bryophyte and associated canopy soil biomass in the cloud immersion zone was estimated at up to 45 t dry mass ha^{-1}, and overall water holding capacity was equivalent to a 20 mm precipitation event. The study emphasizes the importance of diverse bryophyte communities, in sequestering carbon in threatened habitats, with stable isotope analysis allowing future elevational shifts in the cloud base associated with changes in climate to be tracked.

Introduction

Rapid rates of environmental change and population growth are threatening the ecological equilibrium of tropical ecosystems (1), particularly for tropical montane cloud forests (TMCF) (2, 3). Lowland deforestation and increasing temperatures are expected to cause an up-slope shift in the cloud base and thereby disrupt the unique climatic conditions of TMCF formations (4, 5), however the exact location of the cloud base is difficult to identify. TMCFs are biodiversity hotspots, with a high level of endemism and genetic diversity (4, 6-8), but only comprise a small proportion of tropical montane forest area (6.6%: (9)). The specialised TMCF epiphyte flora is dominated by bryophytes (primarily liverworts and mosses): basal land plant groups that cannot control vegetative thallus water use via stomata, and require frequent re-wetting through cloud immersion, precipitation and through-

fall. TMCF habitats are characterised by cool temperatures and constant high relative humidity (10, 11): interception and deposition from fog can contribute over 75% of total precipitation (9). TMCF areas provide important ecosystem services, including protection against soil erosion, stabilization of streamflow and provision of high-quality water for downstream populations, as well as tourism (1, 9, 12), however conservation efforts generally focus on more charismatic taxa in accessible areas.

Due to the difficulties of access and identification, few detailed investigations have been completed on the epiphytic bryophytes of cloud forests. We compiled a detailed inventory of epiphytic bryophytes from an elevational transect in Peru, and exploited the physiological capabilities of bryophytes to establish the current status of these largely unknown, challenging habitats and to assess the future resilience of the forests to potential upshifts in the cloud base. We hypothesize that the stable isotope composition of bryophytes will provide a taxon independent index for the current lower limit of cloud immersion, and that within the cloud immersion zone (CIZ) epiphytic biomass and associated canopy organic matter forms a significant component of canopy biomass, relative to the low lands. Consequently, epiphytic biomass will be a significant store of carbon and water within the cloud immersion zone, that helps maintain the community against extreme precipitation and disturbance.

Materials and Methods

Field sites

In research allied with the Andes Biodiversity and Ecosystem Research Group (ABERG) (13), nine forest plot sites were sampled three times in 2009 along a c.240 km transect from 200 m above sea level (asl) in the Amazon lowland tropical rainforest (LTRF) to the tree line at 3600 m asl on the east slope of the Peruvian Andes (Kosñipata Valley; Fig. 1, Table S1). Meteorological records show a decline in

mean annual temperatures (MAT) with elevation (Fig 1c). Vapor pressure deficit (VPD) declines rapidly to almost 0 kPa at approx. 2000 m asl. Mean annual precipitation (MAP) varies between 1750 mm and 3000 mm (Fig 1d).

Host tree selection and canopy access

During each collecting trip one tree per elevation was selected for canopy access using a 'random-walk' procedure where one set of random numbers (1-360) determined the direction and a second (0-90) the steps walked in the defined direction away from a central point. The host tree was the nearest tree to the endpoint that complied with safety guidelines for canopy access using the double rope technique. Sample collecting was completed at four strata: trunk at head height (HH), lower (LC), mid (MC), and upper crown (UC).

Isotope analysis

During each trip three replicates of each of two most abundant epiphytic moss and liverwort species were collected at each of the four strata in the 27 sampled trees, i.e. 24 samples per accessed tree. Furthermore, two replicate sets of voucher specimens were collected for taxonomic determination. These samples were air dried, catalogued and stored in paper packets for analysis at the Smithsonian Tropical Research Institute (Panama). Isotope analysis was carried out at the Godwin Laboratory (Department of Earth Sciences, University of Cambridge). 0.5–0.75 mg aliquots of dried and milled plant material (188 samples) sealed in silver capsules were used for $^{18}O/^{16}O$ analyses by pyrolysis. The analysis was undertaken by EA-IRMS at using a Thermo Finnigan TC/EA attached to a Thermo Delta V mass spectrometer via a ConFlo 3. The precision of analyses is better than 0.4‰. 0.5–0.75 mg aliquots of the plant material (188 samples) sealed in tin capsules were used for $^{13}C/^{12}C$ and C:N analysis by combustion using a Costech Elemental Analyser attached to a Thermo MAT 253 mass spectrometer. Precision of analyses is better than 0.1‰ for $^{12}C/^{13}C$.

$\delta^{13}C$ values in bryophytes

A fractionation of -4.4‰ is associated with diffusion of CO_2 in air, whilst fractionation associated with liquid phase diffusion is around -1.1‰. Consequently, if CO_2 supply was maximally constrained by diffusion, the measured $\delta^{13}C$ would shift from the atmospheric source CO_2 value (-8 ‰) to -13.5 ‰. Conversely, with unlimited CO_2 supply the maximum theoretical fractionation associated with Rubisco, -27 ‰, could be expressed so the offset including source CO_2 would find tissues of -35 ‰. The typical range of $\delta^{13}C$ values for C3 plants is -22 to -30 ‰. In bryophytes, the the external water layer plays a significant role in determining the extent of fractionation against $^{13}CO_2$ as it limits the rate of diffusion from the atmosphere to chloroplast. Those more limited by diffusion (more closed stomata for C3 vascular plants, more surface liquid in bryophytes) tend to be at the less negative end of the $\delta^{13}C$ range, those where diffusion is less limiting (more open stomata for C3 vascular plants, less surface liquid in bryophytes) tend to have more negative $\delta^{13}C$ values.

Epiphytic cover and surface organic matter collections

Bryophyte epiphytic diversity and biomass was quantified at the four canopy strata using a fixed-effort approach in which one hour was spent collecting all the visible species / morphotypes and all epiphytic material was removed from two 15 cm x 15 cm quadrats, giving a total of 24 quadrats at each elevation. Relevant botanical, ecological and biometric details (circumference of trunk at breast height (*cbh*), tree height (ht_{tot}), height to first branch (ht_1), number of principal branches (*n*) and lengths of principal branches (ht_{br})) about the host tree were recorded as well as percentage cover of each component. Plot census data of all trees were provided by ABERG (for the Andean plots (950–3600 m) and from ACCA (Asociación para la Conservación de la Cuenca Amazónica), Dr. Swamy (Duke University) and RAINFOR (University of Leeds) for the lowland plots (200–300 m). Tree surface areas were calculated from biometric measurements and allometric equations (Table S2, Fig. S1). Epiphyte specimens were separated into lifeform assemblages and morphotypes, for subsequent naming to family or, where possible to genus and species, using macro- and micro-morphometric analyses and

keys (14, 15) and comparisons to herbarium reference collections.

The organic matter in each sample quadrat was removed, bagged, weighed ('field weight'), and whilst fresh, divided into its components. In total 24 organic matter samples were collected at each elevation and 216 along the entire transect. Prior to drying, each organic matter component was used for laboratory-based measurements of maximum water content (MWC), defined as:

MWC = 100*(sw-dw)/dw, [Eqn 1]

where sw is saturated weight of biomass, and dw is dry weight of biomass.

Saturated weight (*sw*) was obtained by submerging the organic matter in water for 30 min, leaving it to drip for 30 min and subsequently weighing. Dry weight (*dw*) of each sample was determined after drying in an oven at 70°C for 48-72h.

Tree allometry and calculation of tree surface area

Mean values of total tree height (ht_{tot}), dbh and the calculated A_{host} of three host trees at each elevation are listed in Table S2. To simplify the calculations of surface area of each host tree (A_{host}) we assumed that trees had a modular structure, composed of a cylinder (trunk to first branch) with other principal branches represented as a series of cones. Using the measured host tree parameters, the surface area of each host tree was calculated [Eqn 2]:

$$A_{host} = ht_1 \times cbh \times \sqrt{(ht_{tot} - ht_1)^2 + \left(\frac{cbh}{2\pi}\right)^2} + n \times \frac{c_{br}}{2} \times \sqrt{(l_{br})^2 + \left(\frac{cbh}{2\pi}\right)^2} \qquad [Eqn\ 2]$$

Where: ht_{tot} is total tree height, ht_1 is height from ground level to first principal branch, l_{br} is length of principal branches, *cbh* is circumference at breast height, c_{br} is average circumference (measured at base) of principal branches and *n* is the number of principal branches.

By correlating the calculated surface areas (A_{host}) with dbh (derived from measured *cbh*) of all host

trees a 'Tree A-dbh model' was derived from the best-fit regression equation (Eqn 3, Fig S1). Subsequently, in conjunction with the available plot census data ($dbh_{tree(i)}$) our model (Eqn 3) was used to compute the tree surface area ($A_{tree(i)}$) of each tree (*i*) with dbh > 10 cm in each forest plot along the Amazon–Andes transect [Eqn 3]

Finally, total tree surface area ($\mathbf{A_{plot(N)}}$) for each 1 ha plot was the sum of the modelled tree surface areas of each tree ($A_{tree(i)}$) (Table S2) (Eqn 4).

$$A_{tree(i)} = -5.16 + 6.68^{0.006 \times dbh_{tree(i)}} + 6.63^{0.03 + dbh_{tree(i)}} \quad [Eqn\ 3]$$

$dbh_{tree(i)}$ diameter of trunk at breast height of each tree (*i*) with dbh > 10cm in each plot.

$$A_{plot(N)} = \sum_{i=1}^{N} A_{tree(i)} \quad [Eqn.\ 4]$$

Upscaling epiphytic organic matter

In order to upscale the epiphytic organic matter measured in each sample quadrat (*bmQ*) to total surface organic matter per tree (*bmT*) it was necessary account for the percentage cover of the individual components on the entire host tree (*cT*) (Fig. 4a). By relating the recorded epiphytic cover in each quadrat (*cQ)* to the visually estimated percentage cover of each organic matter component on the entire host tree (*cT)* a factor *cf* was derived for each host tree (Eqn 5). Subsequently, the *cf* was used to compute the mass of organic matter on each host tree (*bmT*) (Eqn 6).

$$cf_j = \frac{cT}{cQ_j} \quad [Eqn.\ 5]$$

Where: cf_j is cover factor, *cT* is percentage epiphytic cover on entire host tree, *cQ* is percentage epiphytic cover in 15x15 m^2 quadrat.

$$bmT = bmQ \times cf \quad [Eqn.\ 6]$$

173 Where: *bmT* is epiphytic biomass of entire host tree and *bmQ* is epiphytic biomass in 15x15 m^2
174 quadrat.

175 Using the cover factor (*cf)* prevented any under or over represented biomass components in
176 the individual sample quadrats giving rise to erroneous tree-level estimates (*bmT*), which were
177 subsequently used for up scaling of total epiphytic surface organic matter at the stand-level. By using
178 the 'Tree A-dbh model' (Eqn 3) (Fig. S1) and thus knowing the total tree surface area per 1 ha of land
179 (A_{plot}) at each elevation (Table S2) we were able to express the tree-level biomass estimates (*bmT*) at
180 the stand-level, i.e. as tonnes of dry epiphytic organic matter per ha of forest (Fig 5b).

Results

Using stable isotope composition as a climate index

Independent of species, bulk plant $\delta^{13}C$ became less negative from the lowlands (-33‰) to 3000 m asl (-27‰), before becoming more depleted at the highest elevation site (3600 m asl, -29‰, Fig. 2a). Less depleted $\delta^{13}C$ values were associated with lower mean annual vapour pressure deficits (MAVPD, Fig. 2b, Cor = -0.66, r^2=0.43, p<0.0001, df=160), and $\delta^{13}C$ was inversely correlated with nitrogen content, shown as C/N ratio (Fig. 2c, cor = 0.64, r^2=0.40, p<0.0001, df=185). Organic $\delta^{18}O$ was also correlated with MAVPD (Fig. 2d, Cor = 0.53, r^2=0.28, p<0.0001, df=187) with the humid, high elevation sites experiencing lower evaporative enrichment than the Amazon basin (c. 17‰, compared with >18‰).

In order to establish any significant divisions in the bryophyte characteristics, *k*-means cluster analysis was completed to divide the stable isotope and CN data into two clusters, which was determined to be optimal from 30 indices. Consequently, all bryophyte samples collected at elevations lower than 940 m fell into group 1, and all those collected at elevations higher than 2000 m asl in to group 2. For the site at 950 m asl, 21 of the 24 samples fell into group 1, whereas at 1500 m asl 10 of the 24 samples fell into group 2. This clustering, which is taxon independent, corresponds to the extent of diffusion limitation experienced by the epiphytic bryophytes, and thus acts as a index of the extent to which they experience cloud immersion. The division between the two clusters coincides with the significant drop in VPD measured at 2000 m asl (Fig 1c). At low elevation, there is high discrimination against $^{13}CO_2$ (more negative $\delta^{13}C$ values), and more evaporative enrichment of ^{18}O, indicative of rapid diffusion and a leaf surface with a minimal or absent external water layer: at elevations <1000 m the bryophytes do not experience cloud immersion. Above 2000 m the isotope values indicate less discrimination against $^{13}CO_2$ (less negative $\delta^{13}C$ values), and less evaporative enrichment of ^{18}O in leaf organic matter, corresponding to diffusion limitation due to the constant presence of an external water layer through cloud immersion. With 87.5% samples at 1000 m asl in cluster 1, the elevation is likely to be largely cloud free, but the 1500 m asl site with 42% values in cluster 1 and 58% in cluster

2, corresponds to transitional zone of cloud immersion that is periodically inundated but does not experience the persistent cloud immersion of the higher elevation sites. Thus the stable isotope compositions of epiphytic bryophytes provide a quantitative, taxon independent definition for the extent of the cloud immersion zone, the transitional cloud zones and regions which never experience cloud immersion, which is relevant to the interpretation of epiphyte biodiversity patterns.

Bryophyte biodiversity within tropical forest canopies

Overall, the taxonomic analysis revealed 221 liverwort species (spp) (from 75 genera and 25 families) and 84 moss spp (from 60 genera and 21 families; Table S4). This exceeds the 171 spp from 16 families recently reported in the Eastern Andes of Central Peru (16): this was without canopy access, showing the importance of collecting at the tops of the trees, despite the logistical difficulties it entails. Together, these two studies highlight the very high diversity of bryophytes, particularly in cloud-forest formations.

When species richness was expressed independent of tree size, the highest diversity of epiphytic bryophytes across the 3 sampled trees was identified at 1500 m asl (114 spp., Lower Montane Cloud Forest (LMCF)): the climatically sensitive transition into the full cloud immersion zone (Fig. 3a). When normalized by tree surface area, three sites (2000 m asl, 2500 m asl, 3000 m asl) with persistent cloud immersion had the highest epiphytic bryophyte species density (Fig. 3b), over twice that of the sites in the transitional cloud zones (1500 m). The highest elevation site (3600 m) has lower species density: despite having isotopic signals compatible with full immersion, at this high elevation the cooler climate is likely to limit the extent of bryophyte colonization. The sites below 1000 m did not experience cloud immersion, and bryophyte species diversity decreased gradually with elevation from the sub-montane forest to the Amazon lowlands (Fig. 3b). The lowest species diversity was recorded in the lowland sites, with only 29 spp in the terrace forest (300 m asl) and 49 spp in the flood plain forest (250 m asl; Fig. 3a). These values are comparable to the 46 and 86 liverwort species recorded from four trees in the

Peruvian lower and upper montane forest, respectively (17).

Liverwort taxa were dominant throughout the transect, contributing over 80% of species recorded in the UMCF (Table S5). In the lowlands, over 95% of the liverworts were from a single family: the Lejeunaceae (Table S6). The Dicranaceae dominated the moss flora of the high elevation forests, but were absent from the lowland Amazonian sites, where the Sematophyllaceae, Calymperaceae, and Neckeraceae were the most diverse families.

Epiphyte organic matter and water retention capacity

The dominance of bryophyte and canopy soil biomass in the MC and LC profile sections within forest with persistent cloud immersion was striking (Fig 4b, c), relative to lower elevation forest. Vascular epiphytic biomass was highest at all tree strata within the cloud immersion zone. The MC and LC epiphytic biomass reached a maximum of c.4.5 kg m^{-2} at 3000 m asl (Fig. 4). At the highest elevation site (3600 m), samples at head height (HH) held the highest epiphytic biomass (c.3 kg m^{-2}) across the tree profile, elsewhere the epiphyte biomass at HH on tree trunks was much less than the higher canopy strata (Fig. 4d), this maybe due to the reduced stature of the canopy at 3600 m asl, or that the HH strata provides a more sheltered habitat as compared with lower elevations.

In the lowlands, approximately 50% of tree bark remained bare, with highly dispersed and localized epiphytic distributions covering 10–20% of the tree surface (Fig. 5a). Generally increasing with elevation, the highest epiphytic cover of bryophytes (60–80%) and vascular plants (30–40%) coincided within the central cloud immersion zone (CIZ) at 2500–3000 m asl. At the stand level, maximum epiphyte and canopy soil dry biomass was found at the sites with persistent cloud immersion,

equivalent to a total of c.45 Mg DW ha^{-1} at 3000 m asl (Fig. 5b). Approximately 50% of the total epiphytic load was composed of canopy soil, which represented the dominant biomass constituent on trees, particularly in the cloud forest. Within the central CIZ bryophytes and vascular epiphytes each contributed 10–15 Mg DW ha^{-1}, however, outside the CIZ vascular plants constituted less than 5 Mg ha^{-1}. The lowest values were recorded in the lowland tropical rainforest (LTRF), where the development of vascular plants and associated canopy soil was restricted to c.1 Mg ha^{-1}, and bryophytes less than 0.5 Mg ha^{-1}.

Potential water retention capacity (Fig. 5c) was calculated by combining the stand-level estimates of epiphytic biomass (Fig. 5b) with the saturated water capacity of each component, as measured following harvest. The highest water holding capacity by epiphytic biomass was identified at 2500 m asl and was equivalent to a 25 mm rain event, with 80% water retained by canopy soil and the living bryophyte mat. Vascular epiphytes (excluding bromeliad tanks) played a minor role in total canopy water storage (<5 mm). Potential water storage capacity showed a marked drop below 2000 m asl. The substantial and diverse epiphytic biomass of the cloud immersion zone can potentially hold 15–25 times more water than the epiphytes and associated organic matter in the Amazon lowlands. The epiphyte colonization as percentage cover (Fig 5a), biomass combined with canopy soil per unit area (Fig 5b) and water holding capacity (Fig 5c), probably reflect the changing gradients of light availability, temperature, evaporative demand and water replenishment within each tree canopy along the elevational gradient.

Discussion

Environmental forcing, through increasing atmospheric CO_2, changing temperatures, precipitation frequency and intensity, as well as the occurrence of fire and land use change, are having significant and complex effects on Amazonian ecosystems (18), but these effects are difficult to accurately quantify without a complete understanding of the current status of the entire biome. Tropical montane cloud forests are biodiversity hotspots (4, 6-8), yet the bryoflora is poorly characterized (16). Thus, this detailed assessment identifying over 300 bryophyte species along a 3400 m elevational transect makes an important contribution towards providing a more detailed forest inventory, in addition to quantifying the extent of epiphytic biomass and revealing the potential for use of a stable isotope index to track the cloud base.

Stable isotope composition of bryophytes defines the cloud immersion zone

The more enriched $\delta^{13}C$ values (-26.8 to -27.6‰) at 2500–3000 m asl in the Andes, were consistent with CO_2 uptake limited by diffusion due to surface liquid water (19), and carboxylation sink strength limited by low N content (20). For liverwort and moss epiphytes from lowland Amazonia, higher mean annual temperatures lead to increased evaporative demand, and a high MAVPD. Such lifeforms are likely to cycle quickly between dry and rehydrated states, and lose surface water rapidly. In the lowland forests, bryophytes experience less liquid phase diffusion limitation and maximise photosynthetic carbon uptake (and have higher carboxylation capacity as N content) leading to higher carbon isotope fractionation and more negative $\delta^{13}C$ values (19). This interpretation is supported by epiphyte $\delta^{18}O$ signals, with higher evaporative enrichment in tissue water leading to photosynthate incorporated into organic material during growth being relatively enriched in ^{18}O in the lowland epiphytes. One further climatic factor contributing to the differential in $\delta^{18}O$ signals between the high and lowlands is the possible extent of water vapour exchange under high humidity and low MAVPD conditions in the CIZ zone which shifts tissue water, and newly synthesized organic material, towards that of the source precipitation input signal (21). The partial pressure of CO_2 declines with altitude,

and is associated with less negative $\delta^{13}C$ values at altitude in vascular plants (c. 1.1‰ / 1000 m (22)) and bryophytes (1.4-1.8‰ / 1000 m (23)). Whilst changes in partial pressure contribute to the observed 6‰ shift in measured $\delta^{13}C$, it is insufficient to account for all the variation, nor explain the non-linear response of $\delta^{13}C$ to altitude.

The separation of stable isotope and CN values into clusters that are physiologically explicable by the absence, intermittent presence, or permanent presence of a cloud layer, and comparable with the decline in VPD upholds our first hypothesis. As the isotope signals are niche- rather than taxon-specific, as the cloud base moves, the isotope composition of new bryophyte growth will reflect that of the new cloud-free conditions. A change in stable isotope composition therefore has the potential to reveal a shift in the cloud base even before any change in diversity associated with the new environmental conditions.

Epiphytic bryophytes: the hidden diversity of cloud forests

Being hidden in the canopy (24) and consequently often only accessible through tree falls (16), epiphytes are rarely included in forest inventories (25) and therefore much bryophyte diversity remains unidentified and unquantified. Following extensive tree climbing and detailed sampling the identification of 130 species of bryophyte within the cloud immersion zone, almost half of the total along the whole transect and comparable to the diversity of Colombian cloud forests (135 spp; (26)), whilst exceeding that of Costa Rica (96 spp; (27)), emphasises the critical role of cloud forests as biodiversity hotspots. The northern Andes are a liverwort hotspot, with high endemism, hence liverworts dominate moss species particularly at high altitudes with continuous water availability and high humidity (28). Liverworts are generally more susceptible to moisture fluctuations than mosses, which are able to thrive in more disturbed, open and varied forests (28, 29).The elevational trends of species richness, taxon diversity, and life form dominance along the Amazon–Andes gradient show that distinct bryophyte assemblages were found in the zones in which cloud cover

was absent, persistent and transitory, as defined by the stable isotope composition.

Epiphytic bryophytes are significant biomass components in high elevation cloud forests

Ecosystem biomass calculations usually focus on trees (30, 31) and the contribution of epiphytes to canopy structure and function is difficult to quantify via remote sensing (32). Across the Peruvian transect, tree biomass declines above 1500 m asl (13, 33), however vascular epiphytes have a high abundance in the wetter, cloudier conditions of the mid-elevation forests, as was previously observed in Mexico (34), Costa Rica (35), China (36) and across the Andes (37). In contrast, this study shows that biomass of epiphytic bryophytes and arboreal canopy soil peaked at cooler, higher elevations. These differences in biomass accumulation highlight the distinct optimal climatic conditions required for maximum productivity of bryophytes and vascular plants (38, 39). Within trees, the highest accumulation of epiphytic biomass was found in the lower canopy as the large branches and open branch forks facilitate the accumulation of canopy soil and subsequent establishment and growth of plants (40). Smaller epiphytes with less associated canopy soil were typical of the higher canopy strata, due to the reduced area available for colonisation.

Previous estimates of above ground biomass in the same Peruvian cloud forest of 51-89 Mg C ha^{-1} above 2000 m asl (41) and a mean for 3000-3630 m asl of 63.4 Mg C ha^{-1} (25) do not include epiphytic biomass. Assuming that the measured epiphytic biomass is 50% carbon, the 30-50 Mg C ha^{-1} estimated above 2000 m asl is a significant, and unaccounted for component of above ground biomass. Carbon budgets for the cloud forests remain incomplete without inclusion of epiphytic biomass, and counter to some extent the declining net productivity of trees between sub-montane and montane forests (41).

Water holding capacity of bryophytes

In addition to a role in the cloud forest carbon cycle, the water holding capacity of epiphytic bryophytes is significant. In the cloud forests of La Réunion Island (Mascarenes), the water holding

capacity of the epiphytic bryophytes was calculated to be equivalent to a 5 (+/- 2) mm rain event (42), similar to the potential values estimated in this study. Moisture derived from fog precipitation and stored by bryophytes has been estimated to exceed total annual rainfall by 50–90% (43-46), with the storage function of epiphytic biomass more important in seasonally drier areas, such as the SACF (3600 m asl). Thus, it can be expected that the interception and subsequent slow release of moisture during the drier periods can make an important contribution to the hydrological conditions of this forest, where it is unlikely that the groundwater reservoir can sustain the observed dry-season river flow (47) and changes to the hydrological regime can increase the risk of landslides.

Ecosystems at risk: disturbance of cloud forests

TMCF ecosystems are dynamic, with landslides removing c. 6 tC km^{-2} yr^{-1} of vegetation from the Kosñispata Valley (48). In 2010 a single storm triggered 185 landslides (48), most of which were below 1800 m asl, coinciding with the change in stable isotope composition (Fig 2), a significant decrease in epiphytic biomass (Fig 3) and a notable change in forest architecture. Deforestation of the lowland forests is predicted to lead to a reduction in cloud generation and consequently an irreversible loss of the adjacent cloud forest (5), which would have negative effects on canopy biota (49). The current study predicts that an upslope migration of the cloudbank in response to environmental change would lead to a significant decrease in epiphytic biomass, reflecting the decline in epiphytic biomass that coincides with the change in stable isotope composition associated with the transition from permanently cloudy conditions: fitting with transplant experiments in which, amongst a complex set of responses due to the highly heterogeneous nature of the ecosystem, vascular epiphytes moved down slope to warmer, drier environments were small and had reduced recruitment (50). Over time, this would have critical knock-on effects on the accumulation of crown canopy soil and establishment of vascular epiphytes as well as nutrient cycles (51). By regulating the seasonal release of precipitation in the rainy season and providing flood and erosion control, epiphyte mats can play a vital role as ‘capacitors’ in montane forest (3, 49, 52).

Following disturbance it takes approx. 30 years for 100% vegetation cover to return (48), and at least 200 years for the forest to reach maturity (53), though epiphyte recovery can be even slower (54). Stable isotope analysis of bryophyte organic matter provides a clear i for cloud forest zones and the δ^{13}C-C/N-δ^{18}O relationship can serve as a climatic proxy for monitoring of cloud forest limits over time, especially as the cloud base is predicted to move upslope in response to increasing global warming and anthropogenic activities. The lower photosynthetic rates of cloud forest bryophytes as indicated by the reduced rates of isotope discrimination corresponds to slow growth rates and emphasises the particular sensitivity of these species to environmental changes.

References

1. Laurance WF. Emerging threats to tropical forests. Treetops at Risk: Challenges of Global Canopy Ecology and Conservation2013. p. 71-9.
2. Pounds JA, Fogden MPL, Campbell JH. Biological response to climate change on a tropical mountain. Nature. 1999;398:611.
3. Still CJ, Foster PN, Schneider SH. Simulating the effects of climate change on tropical montane cloud forests. Nature. 1999;398:608.
4. Bubb P, May I, Miles L, Sayer J. Cloud Forest Agenda. Cambridge, UK: UNEP-WCMC; 2004.
5. Lawton RO, Nair US, Pielke RA, Welch RM. Climatic Impact of Tropical Lowland Deforestation on Nearby Montane Cloud Forests. Science. 2001;294(5542):584.
6. Gentry AH. Diversity and floristic composition of Andean forests of Peru and adjacent countries: implications for their conservation. Memorias del Museo de Historia Natural, UNMSM (Lima). 1992;21:11-29.
7. Myers N, Mittermeier RA, Mittermeier CG, da Fonseca GAB, Kent J. Biodiversity hotspots for conservation priorities. Nature. 2000;403:853.
8. Bruijnzeel LA, Hamilton LS. Decision Time for Cloud Forests. Paris, France.: UNESCO Division of Water Sciences; 2000.
9. Bruijnzeel LA, Scatena FN. Hydrometeorology of tropical montane cloud forests. Hydrological Processes. 2011;25(3):319-26.
10. Foster P. The potential negative impacts of global climate change on tropical montane cloud forests. Earth-Science Reviews. 2001;55(1):73-106.
11. Fahey TJ, Sherman RE, Tanner EVJ. Tropical montane cloud forest: environmental drivers of vegetation structure and ecosystem function. Journal of Tropical Ecology. 2015;32(5):355-67.
12. Holder CD. The hydrological significance of cloud forests in the Sierra de las Minas Biosphere Reserve, Guatemala. Geoforum. 2006;37(1):82-93.

13. Malhi Y, Silman M, Salinas N, Bush M, Meir P, Saatchi S. Introduction: Elevation gradients in the tropics: laboratories for ecosystem ecology and global change research. GCB. 2010;16(12):3171-5.
14. Gradstein SR, Churchill S, Salazar-Allen N. Guide to the bryophytes of tropical America. New York, USA: NYBG Press; 2001.
15. Gradstein SR, Costa DP. The Hepaticae and Anthocerotae of Brazil. New York, USA: NYBP Press; 2003.
16. Graham JG, Fischer MJ, Tamas P. Bryoflora and landscapes of the Eastern Andes of Central Peru: I. Liverworts of the El Sira Communal Reserve. Acta Biologica Plantarum Agriensis. 2016;4:3-60.
17. Gradstein SR. Diversity of Hepaticae and Anthocerotae in montane forests of tropical Andes. In: Churchill SP, Balslev H, Forero E, Luteyn L, editors. Biodiversity and conservation of neotropical montane
forest. New York: New York Botanic Garden; 1995. p. 321-34.
18. Zhang K, de Almeida Castanho AD, Galbraith DR, Moghim S, Levine NM, Bras RL, et al. The fate of Amazonian ecosystems over the coming century arising from changes in climate, atmospheric CO<inf>2,</inf> and land use. GCB. 2015;21(7):2569-87.
19. Royles J, Horwath AB, Griffiths H. Interpreting bryophyte stable carbon isotope composition: Plants as temporal and spatial climate recorders. Geochemistry, Geophysics, Geosystems. 2014;15(4):1462-75.
20. Griffiths H, Borland A, Gillon J, Harwood K, Maxwell K, Wilson J. Stable isotopes reveal exchanges between soil, plants and the atmosphere. In: Press MC, Scholes JD, Barker MG, editors. Physiological plant ecology UK: British Ecological Society; 1999. p. 415-41.
21. Helliker BR, Griffiths H. Toward a plant-based proxy for the isotope ratio of atmospheric water vapor. GCB. 2007;13(4):723-33.
22. Körner C, Farquhar GD, Wong SC. Carbon isotope discrimination by plants follows latitudinal and altitudinal trends. Oecologia. 1991;88:30-40.
23. Ménot G, Burns SJ. Carbon isotopes in ombrogenic peat bog plants as climatic indicators: calibration from an altitudinal transect in Switzerland. Organic Geochemistry. 2001;32:233-45.
24. Romanski J, Pharo EJ, Kirkpatrick JB. Epiphytic bryophytes and habitat variation in montane rainforest, Peru. Bryologist. 2011;114(4):720-31.
25. Gibbon A, Silman MR, Malhi Y, Fisher JB, Meir P, Zimmermann M, et al. Ecosystem Carbon Storage Across the Grassland–Forest Transition in the High Andes of Manu National Park, Peru. Ecosystems. 2010;13(7):1097-111.
26. Wolf JHD. Diversity Patterns and Biomass of Epiphytic Bryophytes and Lichens Along an Altitudinal Gradient in the Northern Andes. Annals of the Missouri Botanical Garden. 1993;80(4):928-60.
27. Holz I, Gradstein SR, Heinrichs J, Kappelle M. Bryophyte Diversity, Microhabitat Differentiation, and Distribution of Life Forms in Costa Rican Upper Montane Quercus Forest. The Bryologist. 2002;105(3):334-48.
28. Frahm JP. Manual of tropical bryology. Tropical bryology. 2003;23:1-196.
29. da Costa DP. Epiphytic Bryophyte Diversity in Primary and Secondary Lowland Rainforests in Southeastern Brazil. The Bryologist. 1999;102(2):320-6.
30. Slik JWF, Paoli G, McGuire K, Amaral I, Barroso J, Bastian M, et al. Large trees drive forest aboveground biomass variation in moist lowland forests across the tropics. Global Ecology and Biogeography. 2013;22(12):1261-71.

31. Venter M, Dwyer J, Dieleman W, Ramachandra A, Gillieson D, Laurance S, et al. Optimal climate for large trees at high elevations drives patterns of biomass in remote forests of Papua New Guinea. GCB. 2017;23(11):4873-83.
32. Asner GP, Anderson CB, Martin RE, Knapp DE, Tupayachi R, Sinca F, et al. Landscape-scale changes in forest structure and functional traits along an Andes-to-Amazon elevation gradient. Biogeosci. 2014;11(3):843-56.
33. Girardin CAJ, Malhi Y, Aragão LEOC, Mamani M, Huaraca Huasco W, Durand L, et al. Net primary productivity allocation and cycling of carbon along a tropical forest elevational transect in the Peruvian Andes. GCB. 2010;16(12):3176-92.
34. Hietz P, Hietz-Seifert U. Composition and ecology of vascular epiphyte communities along an altitudinal gradient in central Veracruz, Mexico. Journal of Vegetation Science. 1995;6(4):487-98.
35. Cardelus CL, Colwell RK, Watkins JE. Vascular epiphyte distribution patterns: explaining the mid-elevation richness peak. J Ecol. 2006;94(1):144-56.
36. Ding Y, Liu G, Zang R, Zhang J, Lu X, Huang J. Distribution of vascular epiphytes along a tropical elevational gradient: disentangling abiotic and biotic determinants. Scientific Reports. 2016;6:19706.
37. Salazar L, Homeier J, Kessler M, Abrahamczyk S, Lehnert M, Krömer T, et al. Diversity patterns of ferns along elevational gradients in Andean tropical forests. Plant Ecology & Diversity. 2015;8(1):13-24.
38. Frahm J-P. Bryophyte phytomass in tropical ecosystems. Botanical Journal of the Linnean Society. 1990;104(1-3):23-33.
39. McLaughlin BC, Ackerly DD, Klos PZ, Natali J, Dawson TE, Thompson SE. Hydrologic refugia, plants, and climate change. GCB. 2017;23(8):2941-61.
40. Johansson D. Ecology of vascular epiphytes in West African rain forest. Uppsala, Sweden1974. 1–129 p.
41. Malhi Y, Girardin CAJ, Goldsmith GR, Doughty CE, Salinas N, Metcalfe DB, et al. The variation of productivity and its allocation along a tropical elevation gradient: a whole carbon budget perspective. New Phyt. 2017;214(3):1019-32.
42. Ah-Peng C, Cardoso AW, Flores O, West A, Wilding N, Strasberg D, et al. The role of epiphytic bryophytes in interception, storage, and the regulated release of atmospheric moisture in a tropical montane cloud forest. Journal of Hydrology. 2017;548:665-73.
43. Pócs T. The epiphytic biomass and its effect on the water balance of two rain forest types in the Uluguru Mountians (Tanzania, East Africa). Acta Botanica Acadamiae Scientiarum Hungericae. 1980;26:143-67.
44. Cavelier J, Goldstein G. Mist and fog interception in elfin cloud forests in Colombia and Venezuela. Journal of Tropical Ecology. 1989;5(3):309-22.
45. Jarvis A. Quantifying the hydrological role of cloud deposition onto epiphytes in a tropical montane cloud forest, Colombia: UCL; 2000.
46. Woda C, Huber A, Dohrenbusch A. Vegetación epifita y captación de neblina en bosques siempreverdes en la Cordillera Pelada, sur de Chile. Bosque (Valdivia). 2006;27:231-40.
47. Clark KE, Torres MA, West AJ, Hilton RG, New M, Horwath AB, et al. The hydrological regime of a forested tropical Andean catchment. Hydrology and Earth System Sciences. 2014;18(12):5377-97.

48. Clark KE, West AJ, Hilton RG, Asner GP, Quesada CA, Silman MR, et al. Storm-triggered landslides in the Peruvian Andes and implications for topography, carbon cycles, and biodiversity. Earth Surface Dynamics. 2016;4(1):47-70.
49. Nadkarni NM, Solano R. Potential effects of climate change on canopy communities in a tropical cloud forest: an experimental approach. Oecologia. 2002;131(4):580-6.
50. Rapp JM, Silman MR. Epiphyte response to drought and experimental warming in an Andean cloud forest F1000Research. 2014;3(7):[version 2; referees: approved].
51. Clark KL, Nadkarni NM, Gholz HL. Growth, Net Production, Litter Decomposition, and Net Nitrogen Accumulation by Epiphytic Bryophytes in a Tropical Montane Forest1. Biotropica. 1998;30(1):12-23.
52. Weathers KC. The importance of cloud and fog in the maintenance of ecosystems. Trends in Ecology & Evolution. 1999;14(6):214-5.
53. Dislich C, Huth A. Modelling the impact of shallow landslides on forest structure in tropical montane forests. Ecological Modelling. 2012;239(Supplement C):40-53.
54. Price K, Lilles EB, Banner A. Long-term recovery of epiphytic communities in the Great Bear Rainforest of coastal British Columbia. Forest Ecology and Management. 2017;391:296-308.

Author contributions

Study was conceived by ABH, HG. Fieldsite network was set up by YM, MS. Fieldwork and sample processing were carried out by ABH, RT. Species identification was completed by ABH, JAG, NSA. Plot census data were provided by WF-R, VS, JPLF. ABERG meteorological data were compiled by JMR. Data analysis was completed by ABH, JR. Paper was drafted by JR, ABH, HG.

Acknowledgements

This paper is a product of the Andes Biodiversity and Ecosystems Research Group. We thank Asociación para la Conservación de la Cuenca Amazónica for the use of the Wayqecha and Los Amigos Biological Station, Incaterra (San Pedro) and Pantiacolla Lodge for the use of the land and facilities, Explorers Inn for the use of Tambopata field station, the Manu National Park, INRENA and SERNANP for permission to work in the protected areas. We also thank the Servicio Nacional de Meteorología e Hidrología del Perú and the Botanical Research Institute of Texas for meteorological data. We thank Guido Vilcahuamán Fernández, Israel Cuba Torres, Hilario Recharte Matamoros, José Luis Mancilla Quispe, Tom Middleton, Lizzie Whitebread, and Al Toth for field assistance, Glyn Jones for laboratory support, Eric Horwath and Jamie Males for useful discussions.

Figure Legends

Figure 1. Description of fieldwork sites in Peru a) Location of fieldwork sites in Peru; b) elevational positions of sampling sites within their forest types (Table S1); c) Mean annual temperature, mean annual vapour pressure deficit and (d) mean annual precipitation at nearest meteorological station to each site (Table S3); e) View from 1600 m asl towards the 1500 m asl plots, showing the cloud base/transition zone in April 2008; f) interior of the sub-alpine cloud forest at 3600 m asl.

Figure 2: **Stable isotope composition of bryophyte organic matter across elevational transect** a) Mean $\delta^{13}C$ discrimination measured in epiphytic bryophyte organic matter as a function of elevation (n=188); b) Mean $\delta^{13}C$ as a function of mean annual vapour pressure deficit (MAVPD); c) Mean $\delta^{13}C$ as a function of C/N ratio of bulk epiphytic bryophytes along elevational transect; d) Mean $\delta^{18}O$ as a function of MAVPD. Shading represents the *k*-means data clusters: white background corresponds to locations where all data falls into cluster 1, dark grey corresponds to elevations with all data falling in cluster 2, and the light grey represents locations with a mixture of clusters: clusters and shading also represent extent of persistent cloud immersion from none in white to transitional in light grey and permanent in dark grey.

Figure 3: **Diversity of epiphytic bryophytes in relation to elevation and tree size.** a) Species total collected from 3 trees at each sampling location; b) Species total from 3 trees at each elevation normalised per m^2 bark surface area. Liverworts (triangles), mosses (circles) and total (squares). Shading represents the clusters of isotope data (Fig 2), which relates to the extent of persistent cloud immersion from none in white to permanent in dark grey.

Figure 4: Distribution of epiphytic biomass components, separated between tree strata, across the elevational gradient: a) Upper crown (UC); b) Mid-crown (MC); c) Lower crown (LC) and d) Head Height (HH). Shading represents the clusters of isotope data (Fig 2), which relates to the extent of

persistent cloud immersion from none in white to permanent in dark grey.

Figure 5: **Contribution of epiphytic bryophytes to carbon and water storage** a) Observed epiphytic cover of tree surfaces along the elevational gradient separated by component, n=3 trees per elevation, total epiphytic cover is >100% when biomass components overlap; b) Estimated epiphytic biomass (dry weight) per hectare of forest; c) Potential water storage capacity of epiphytic biomass calculated from saturated water holding capacity. The forest formations at each elevation are defined in the Figure 1, which relates to the extent of persistent cloud immersion from none in white to permanent in dark grey. Error bars represent SE of mean.

Supplementary Data Files

Table S1: Sampling Site Information

Table S2: Mean host tree measurements at each elevation and plot data used for biomass calculations. Host trees: dbh (diameter at breast height) and ht_{tot} (total tree height) were measured in the field (n=3). A_{host} (tree surface area) was calculated using the "Tree A-dbh model", SE given in parentheses. Plots: No stems = total number of stems (>10 cm dbh) per 1 ha forest plot, A_{plot} = total tree area per 1 ha plot, calculated using the "Tree A-dbh model".

Table S3: Summary of meteorological data from weather stations located in close proximity to the sampling sites. MAT: Mean Annual Temperature, MAP: Mean annual precipitation, VPD: Vapour pressure deficit, SENHAMI: Servicio Nacional de Meteorologia e Hidrologia, ABERG: Andes Biodiversity and Ecosystem Research Group, Atrium: database from The Botanical research Institute of Texas * Data collected at 2750 m

Table S4: Number of liverwort and moss species, per genera, recorded across the transect

Table S5: Percentages of moss and liverworts species recorded across altitudinal transect

Table S6: Most abundant epiphytic bryophytes and all vascular plants recorded on three host trees at each elevation

Fig S1. Non-linear regression function ("Tree A-dbh model"), based on allometric calculations and existing plot census data (dbh for all trees >10 cm) used to estimate total surface area in one hectare plot: $y = 7.96e^{0.029x}$

Supplementary Information Continued: Data used for Figures 2-5

Figure 1. Description of fieldwork sites in Peru a) Location of fieldwork sites in Peru; b) elevational positions of sampling sites within their forest types (Table S1); c) Mean annual temperature, mean annual vapour pressure deficit and (d) mean annual precipitation at nearest meteorological station to each site (Table S3); e) View from 1600 m asl towards the 1500 m asl plots, showing the cloud base/transition zone in April 2008; f) interior of the sub-alpine cloud forest at 3600 m asl.

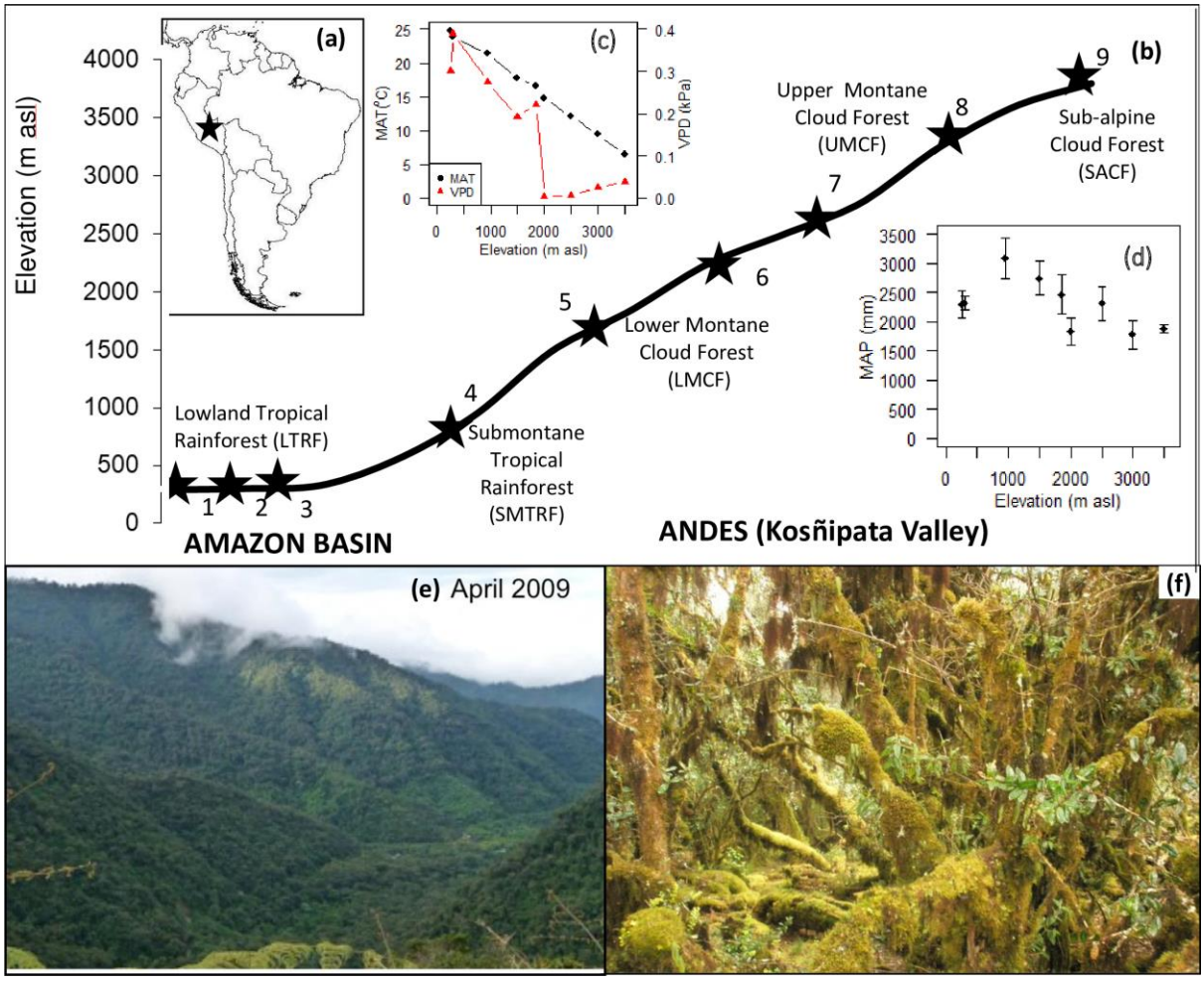

Figure 2: **Stable isotope composition of bryophyte organic matter across elevational transect** a) Mean $\delta^{13}C$ discrimination measured in epiphytic bryophyte organic matter as a function of elevation (n=188); b) Mean $\delta^{13}C$ as a function of mean annual vapour pressure deficit (MAVPD); c) Mean $\delta^{13}C$ as a function of C/N ratio of bulk epiphytic bryophytes along elevational transect; d) Mean $\delta^{18}O$ as a function of MAVPD. Shading represents the *k*-means data clusters: white background corresponds to locations where all data falls into cluster 1, dark grey corresponds to elevations with all data falling in cluster 2, and the light grey represents locations with a mixture of clusters: clusters and shading also represent extent of persistent cloud immersion from none in white to transitional in light grey and permanent in dark grey.

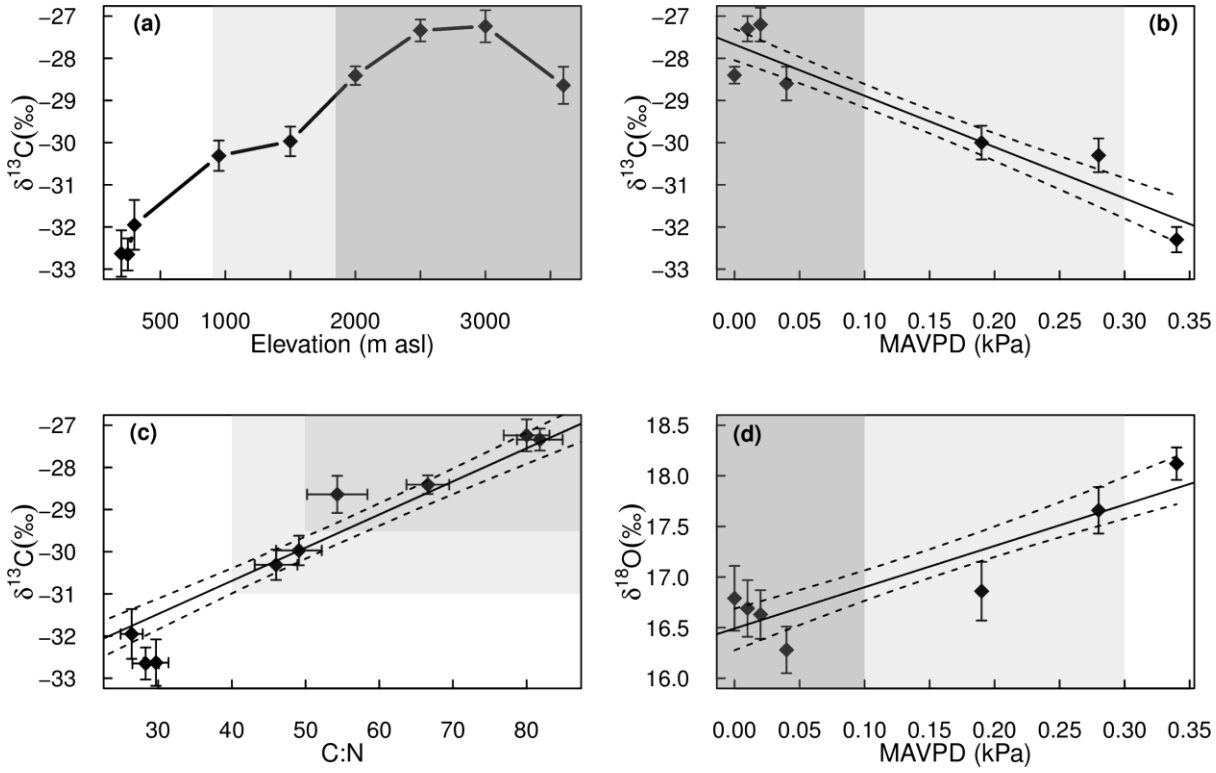

Figure 3: **Diversity of epiphytic bryophytes in relation to elevation and tree size.** a) Species total collected from 3 trees at each sampling location; b) Species total from 3 trees at each elevation normalised per m^2 bark surface area. Liverworts (triangles), mosses (circles) and total (squares). Shading represents the clusters of isotope data (Fig 2), which relates to the extent of persistent cloud immersion from none in white to permanent in dark grey.

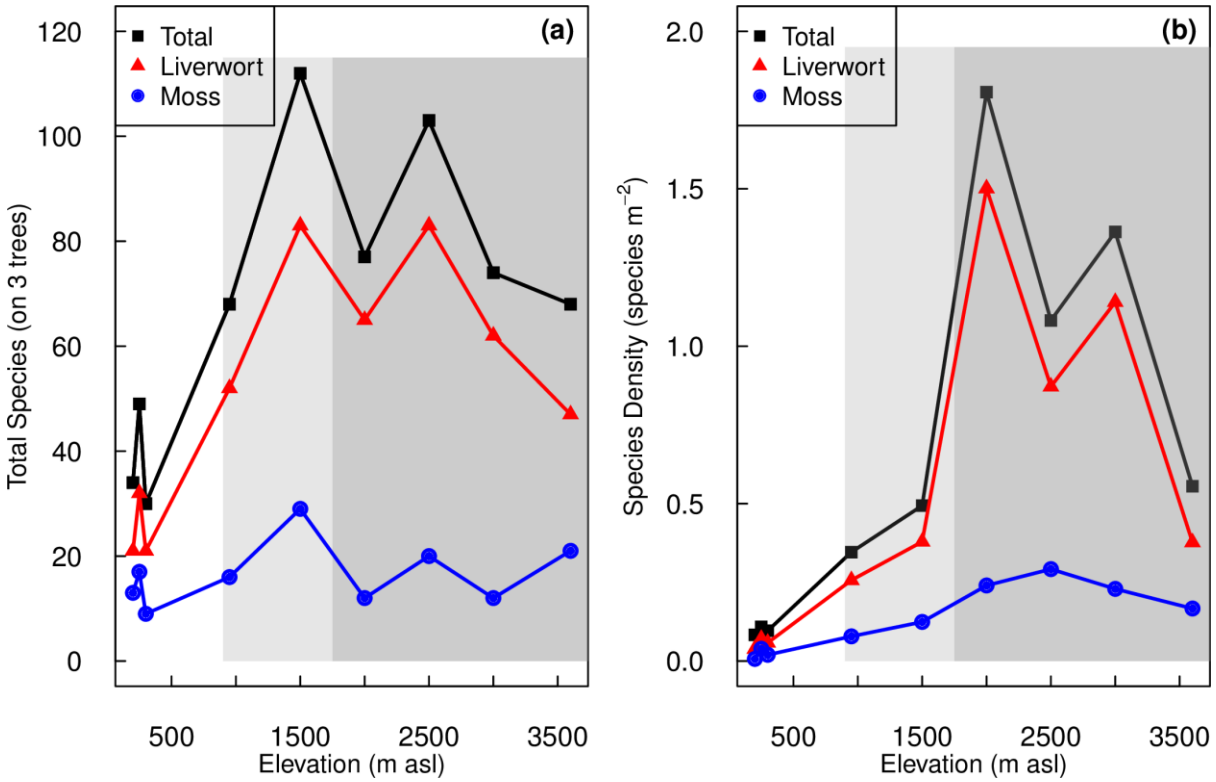

Figure 4: Distribution of epiphytic biomass components, separated between tree strata, across the elevational gradient: a) Upper crown (UC); b) Mid-crown (MC); c) Lower crown (LC) and d) Head Height (HH). Shading represents the clusters of isotope data (Fig 2), which relates to the extent of persistent cloud immersion from none in white to permanent in dark grey.

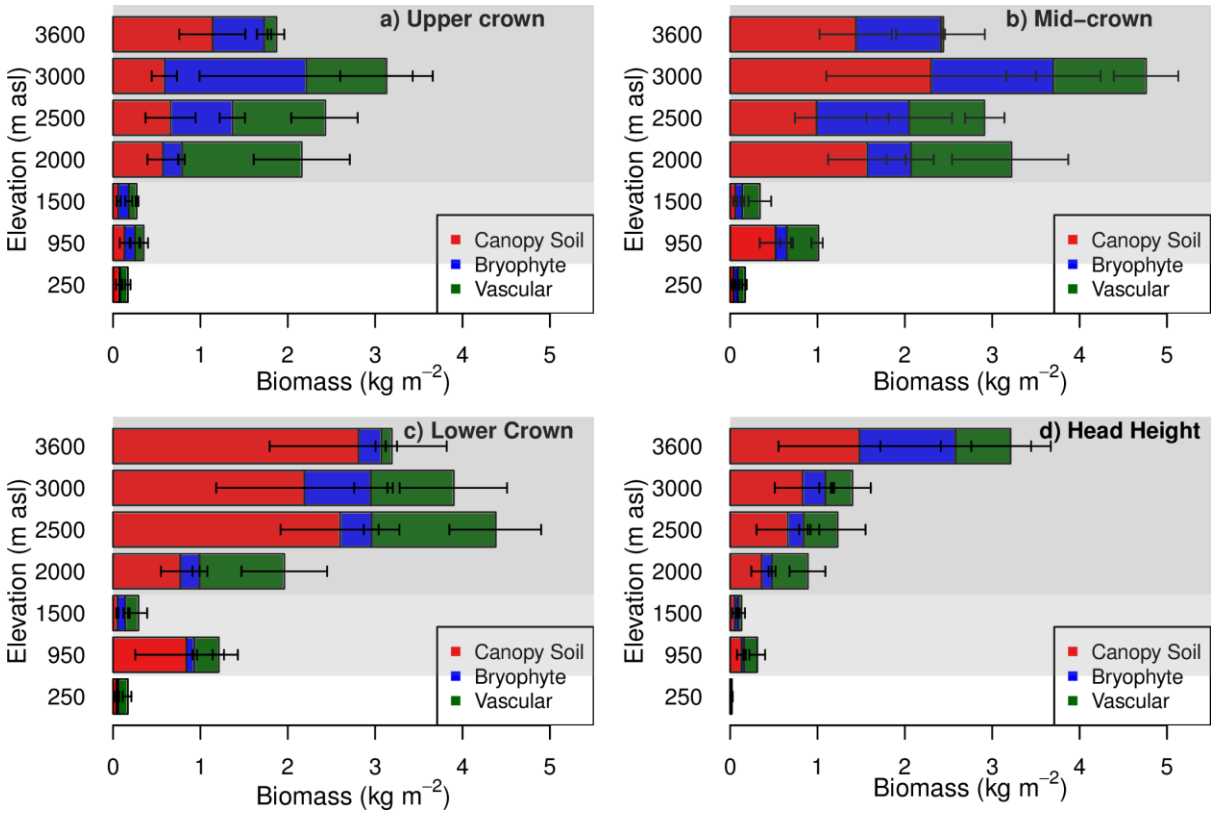

Figure 5: **Contribution of epiphytic bryophytes to carbon and water storage** a) Observed epiphytic cover of tree surfaces along the elevational gradient separated by component, n=3 trees per elevation, total epiphytic cover is >100% when biomass components overlap; b) Estimated epiphytic biomass (dry weight) per hectare of forest; c) Potential water storage capacity of epiphytic biomass calculated from saturated water holding capacity. The forest formations at each elevation are defined in the Figure 1, which relates to the extent of persistent cloud immersion from none in white to permanent in dark grey. Error bars represent SE of mean.

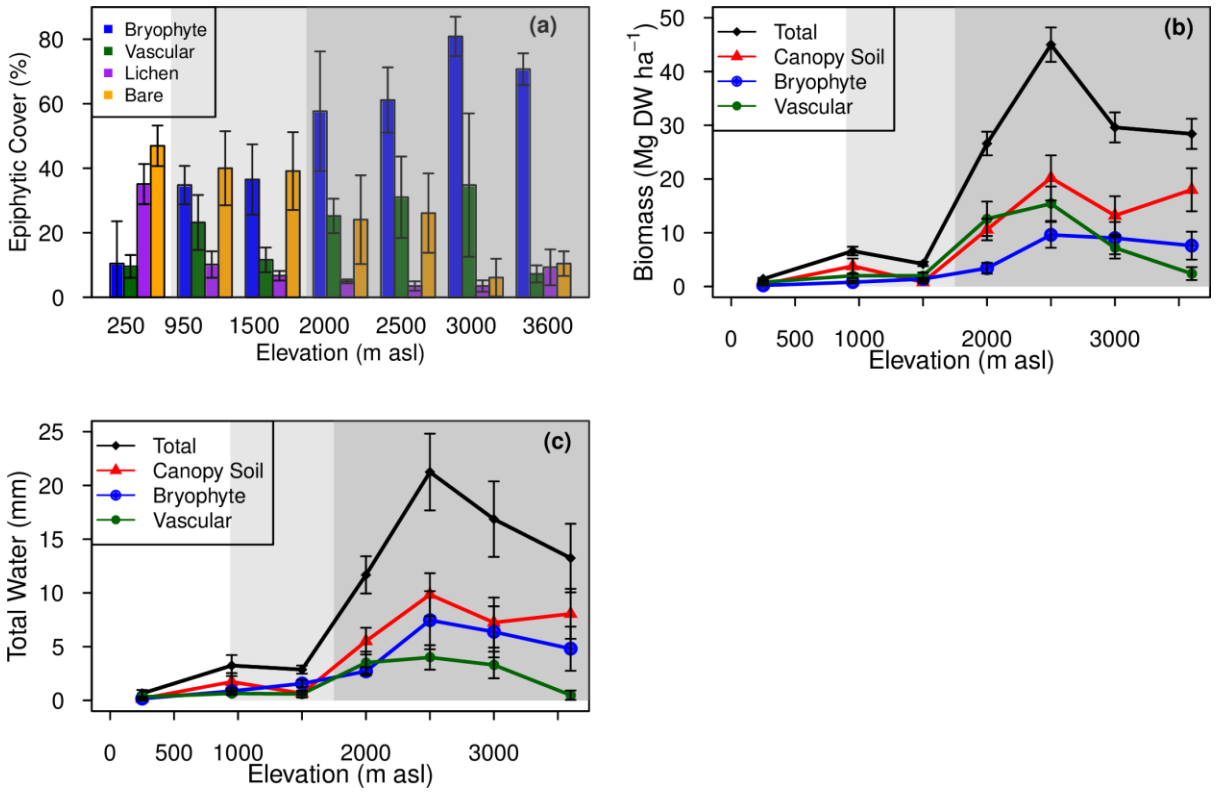

Supplementary Information for:

Bryophyte stable isotope composition, diversity and biomass define tropical montane cloud forest extent

Aline B. Horwath, Jessica Royles, Richard Tito, José A. Gudiño, Noris Salazar Allen, William Farfan-Rios, Joshua M. Rapp, Miles R. Silman, Yadvinder Malhi, Varun Swamy, Jean Paul Latorre Farfan, Howard Griffiths

Proceedings of the Royal Society B

DOI: 10.1098/rspb.2018.2284

Table S1: Sampling Site Information

Table S2: Mean host tree measurements at each elevation and plot data used for biomass calculations. Host trees: dbh (diameter at breast height) and ht_{tot} (total tree height) were measured in the field (n=3). A_{host} (tree surface area) was calculated using the "Tree A-dbh model", SE given in parentheses. Plots: No stems = total number of stems (>10 cm dbh) per 1 ha forest plot, A_{plot} = total tree area per 1 ha plot, calculated using the "Tree A-dbh model".

Table S3: Summary of meteorological data from weather stations located in close proximity to the sampling sites. MAT: Mean Annual Temperature, MAP: Mean annual precipitation, VPD: Vapour pressure deficit, SENHAMI: Servicio Nacional de Meteorologia e Hidrologia (http://www.senhami.gob.pe/), ABERG: Andes Biodiversity and Ecosystem Research Group, Atrium: database from The Botanical research Institute of Texas (http://atrium.andesamazon.org/index), * Data collected at 2750 m

Table S4: Number of liverwort and moss species, per genera, recorded across the transect

Table S5: Percentages of moss and liverworts species recorded across altitudinal transect

Table S6: Most abundant epiphytic bryophytes and all vascular plants recorded on three host trees at each elevation

Fig S1. Non-linear regression function ("Tree A-dbh model"), based on allometric calculations and existing plot census data (dbh for all trees >10 cm) used to estimate total surface area in one hectare plot: $y = 7.96e^{0.029x}$

Supplementary Information Continued: Data used for Figures 2-5

Table S1: Sampling Site Information: Site Code, forest type, altitude, sampling date, Host tree, most common tree, geographical information

Site Code	Forest Type	Alt (m asl)	Date	Host tree species (Family)	Most common tree species	Latitude	Longitude	Geographical Location
TP 200	**Lowland Tropical Rainforest** (LTRF)	210 190 200	13-05-09 23-07-09 05-10-09	*Parkia sp.* (Leguminosae) *Ficus sp* (Moraceae) *Ficus sp* (Moraceae)	*Pourouma minor* (Urticaceae) *Bixa arborea* (Bixaceae) *Pseudolmedia laevigata* (Moraceae) *Roucheria columbiana* (Linaceae) *Iryanthera juruensis* (Myristicaceae)	S12 50' 08.9" S12° 51' 03.4" S12° 51' 29.7"	W69° 16' 46.2 W69° 17' 34.5" W69° 17' 24.8"	Tambopata National Reserve, Explorer's Inn; Puerto Maldonado, Madre de Dios, Peru.
CICRA 250	**Lowland Tropical Rainforest** (LTRF)	240 250 250	17-05-09 17-07-09 30-09-09	*Luehea cymulosa* (Malvaceae) *Clarisia racemosa* (Moraceae) *Sloanea obtusifolia* (Elaeocarpaceae)	*Pseudolmedia laevis* (Moraceae) *Otoba parvifolia* (Myristicaceae) *Quararibea wittii* (Malvaceae) *Theobroma cacao* (Malvaceae) *Oxandra acuminata* (Annonaceae)	S12° 34' 07.5" S12° 34' 09.8" S12° 34' 12.5"	W70° 04' 55.7" W70° 04' 55.4" W70° 04' 54.7"	CICRA-bajio (flood plain forest); CICRA, Colorado, Puerto Maldonado, Madre de Dios, Peru.
CICRA 300	**Lowland Tropical Rainforest** (LTRF)	300 280 280	18-05-09 17-07-09 01-10-09	*Bertholletia excelsa* (Lecythidaceae) *Pouteria sp.* (Sapotaceae) *Hevea cf. brasiliensis* (Euphorbiaceae)	*Pourouma minor* (Urticaceae) *Leonia glycycarpa* (Violaceae) *Cecropia sciadophylla* (Urticaceae) *Pourouma sp* (Urticaceae) *Protium puncticulatum* (Burseraceae)	S12° 33' 07.7" S12° 33' 05.8" S12° 33' 03.7"	W70° 06' 17.0" W70° 06' 15.5" W70° 06' 14.4"	CICRA-terraza (terrace forest); CICRA, Colorado, Puerto Maldonado, Madre de Dios, Peru.
TON-01	**Sub-montane tropical rainforest** (SMTRF)	930 940 950	29-04-09 09-07-09 15-09-09	*Cordia scabrifolia* (Boraginaceae) *Sloanea guianensis* (Elaeocarpaceae) *Cedrelinga cateniformis* (Leguminosae)	*Virola elongata* (Myristicaceae) *Perebea guianensis* (Moraceae) *Cedrelinga cateniformis* (Leguminosae) *Cecropia sp* (Urticaceae) *Neea sp* (Nyctaginaceae)	S12° 57' 31.8" S12° 57' 32.7" S12° 57' 34.1"	W71° 33' 57.7" W71° 33' 58.1" W71° 33' 58.5"	Tono, plot II, Manu National Park (MNP); Patria, Kosñipata, Cusco, Peru.

SPD-02	**Lower Tropical Montane Cloud Forest** (LTMCF)	1500 1530 1500	28-04-09 07-07-09 14-09-09	*Ficus trigona* (Moraceae) *Tapirira obtusa* (Anacardiaceae) *Hieronyma macrocarpa* (Phyllanthaceae)	*Virola sp* (Myristicaceae) *Turpinia occidentalis* (Staphyleaceae) *Tachigali setifera* (Leguminosae) *Myrcia sp* (Myrtaceae) *Inga sp* (Leguminosae)	S13° 02' 57.0" S13° 02' 56.6" S13° 02' 57.8"	W71° 32' 10.9" W71° 32' 13.2" W71° 32' 10.6"	San Pedro, plot II; Paucartambo, Cusco, Peru.
TRU-07	**Lower Tropical Montane Cloud Forest** (LTMCF)	2000 2010 2030	26-04-09 5-07-09 12-09-09	*Alzatea verticillata* (Alzateaceae) *Alzatea verticillata* (Alzateaceae) *Alzatea verticillata* (Alzateaceae)	*Alzatea verticillata* (Alzateaceae) *Ilex villosula* (Aquifoliaceae) *Clusia sp* (Clusiaceae) *Myrcia sp* (Myrtaceae) *Alchornea sp* (Euphorbiaceae)	S13° 04' 27.0" S13° 04' 26.9" S13° 04' 27.2"	W71° 33' 34.4" W71° 33' 33.5" W71° 33' 35.0"	Trocha Union, plot VII, MNP; Paucartambo, Cusco, Peru.
TRU-05	**Upper Tropical Montane Cloud Forest** (UTMCF)	2510 2550 2530	24-04-09 04-07-09 10-09-09	*Clusia trochiformis* (Clusiaceae) *Clethra revoluta* (Clethraceae) *Alchornea grandiflora* (Euphorbiaceae)	*Clusia sp* (Clusiaceae) *Weinmannia bangii* (Cunoniaceae) *Alchornea sp* (Euphorbiaceae) *Myrsine sp* (Primulaceae) *Weinmannia microphylla* (Cunoniaceae)	S13° 05' 37.4" S13° 05' 38.3" S13° 05' 38.0"	W71° 34' 27.6" W71° 34' 26.3" W71° 34' 25.9"	Trocha Union, plot V, MNP; Paucartambo, Cusco, Peru.
TRU-03	**Upper Tropical Montane Cloud Forest** (UTMCF)	3020 3040 3040	23-04-09 02-07-09 09-09-09	*Axinaea pennellii* (Melastomataceae) *Clusia alata (*Clusiaceae) *Persea corymbosa* (Lauraceae)	*Clusia sp* (Clusiaceae) *Clusia alata* (Clusiaceae) *Myrsine sp* (Primulaceae) *Weinmannia microphylla* (Cunoniaceae) *Miconia cataractae* (Melastomataceae)	S13° 06' 32.9" S13° 06' 34.9" S13° 06' 33.7"	W71° 35' 57.3" W71° 35' 58.9" W71° 35' 58.8"	Trocha Union, plot III, MNP Paucartambo, Cusco, Peru.
TC 3600	**Sub-alpine cloud forest** (SACF)	3610 3560 3640	21-04-09 30-Jun-09 07-09-09	*Weinmannia fagaroides* (Cunoniaceae) *Weinmannia cochensis* (Cunoniaceae) *Polylepis pauta* (Rosaceae)	*Polylepis pauta* (Rosaceae) *Weimannia spp* (Cunoniaceae) *Miconia sp* (Melastomataceae) *Ilex sp* (Aquifoliaceae) *Symplocos sp* (Symplocaceae)	S13° 07' 23.0" S13° 07' 23.2" S13° 07' 23.7"	W71° 37' 04.8" W71° 37' 04.6" W71° 37' 03.7"	Tres Cruces, MNP; Acjanaco, Paucartambo, Cusco, Peru.

Table S2: Mean host tree measurements at each elevation and plot data used for biomass calculations. Host trees: dbh (diameter at breast height) and ht_{tot} (total tree height) were measured in the field (n=3). A_{host} (tree surface area) was calculated using the "Tree A-dbh model", SE given in parentheses. Plots: No stems = total number of stems (>10 cm dbh) per 1 ha forest plot, A_{plot} = total tree area per 1 ha plot, calculated using the "Tree A-dbh model".

Altitude (m asl)	Forest Type	HOST TREES			PLOTS	
		dbh (cm)	ht_{tot} (m)	A_{host} (m^2)	No stems	Aplot (ha)
200	Amazon lowland tropical rain forest (LTRF)	100.5 (9.4)	39.0 (3.2)	166.2 (64.3)	535	0.93
250	Amazon lowland tropical rain forest (LTRF)	82.2 (2.4)	42.7 (1.8)	130.3 (7.1)	666	1.2
300	Amazon lowland tropical rain forest (LTRF)	85.0 (8.0)	38.0 (3.5)	101.4 (11.9)	500	0.92
950	Sub-montane tropical rain forest (Sub-MTRF)	65.0 (17.0)	31.7 (4.4)	65.1 (29.2)	450	0.91
1500	Lower montane cloud forest (LMCF)	45.6 (6.4)	20.5 (2.5)	32.8 (5.9)	870	1.59
2000	Lower montane cloud forest (LMCF)	35.3 (2.9)	14.7 (0.9)	14.6 (3.7)	960	1.29
2500	Upper montane cloud forest (UMCF)	33.0 (10.6)	26.3 (3.5)	31.5 (5.7)	1027	1.65
3000	Upper montane cloud forest (UMCF)	33.0 (4.8)	15.3 (1.5)	18.8 (2.5)	593	0.9
3600	Sub-alpine cloud forest (SACF)	71.7 (2.5)	18.7 (3.5)	41.8 (0.8)	647	1.05

Table S3: Summary of meteorological data from weather stations located in close proximity to the sampling sites. MAT: Mean Annual Temperature, MAP: Mean annual precipitation, VPD: Vapour pressure deficit, SENHAMI: Servicio Nacional de Meteorologia e Hidrologia (http://www.senhami.gob.pe/), ABERG: Andes Biodiversity and Ecosystem Research Group, Atrium: database from The Botanical research Institute of Texas (http://atrium.andesamazon.org/index), * Data collected at 2750 m

Altitude (m asl)	MAT (°C)	MAP (mm)	MAP SE (mm)	VPD (kPa)	Met station Location	Latitude (°S)	Longitude (°W)	Source	Period
200	24.7	2299	223	0.302	Pto. Maldonado	12°35'22"	69°12'18"	SENHAMI	2001-2006
250	23.9	2322	119	0.389	CICRA	12°34'09"	70°06'00"	Atrium	2007/08
300	21.4	3086	349	0.275	Tono	12°57'58"	71°33'96"	ABERG	2007/08
950	17.7	2746	294	0.192	San Pedro	13°02'90"	71°32'19"	ABERG	2007/08
1500	16.6	2472	331	0.221	TU VIII	13°04'19"	71°33'35"	ABERG	2007/08
2000	14.8	1828	232	0.003	TU VII	13°04'42"	71°33'56"	ABERG	2007/08
2500	12.1	2318*	292	0.006	TU V	13°06'31"	71°35'36"	ABERG	2007/08
3000	9.4	1776	255	0.024	TU III	13°06'54"	71°35'99"	ABERG	2007/08
3600	6.4	1880	72	0.037	Acjanaco	13°11'46"	71°37'11"	SENHAMI	2001-2006

Table S4: Number of liverwort and moss species, per genera, recorded across the transect

	Altitude (m asl)	200	250	300	950	1500	2000	2500	3000	3600	TOTAL
Liverworts	Acrobolbaceae	0	0	0	0	0	0	1	1	0	2
	Anastrophyllaceae	0	0	0	0	0	1	2	1	2	6
	Aneuraceae	0	0	0	1	2	0	3	4	1	11
	Calypogeiaceae	0	0	1	2	3	2	2	1	0	11
	Cephaloziaceae	0	0	0	3	1	1	2	1	1	9
	Geocalycaceae	0	0	0	2	2	3	4	2	3	16
	Herbertaceae	0	0	0	1	1	2	2	3	2	11
	Icacinaceae	0	0	0	2	2	1	2	2	2	11
	Jubulaceae	0	0	0	1	4	3	1	3	4	16
	Jungermanniaceae	0	0	0	0	1	3	2	3	1	10
	Lejeuneaceae	18	24	16	13	35	24	18	8	10	166
	Lepicoleaceae	0	0	0	0	0	0	3	2	1	6
	Lepidoziaceae	0	0	0	14	8	10	15	12	4	63
	Lophocoleaceae	0	1	0	1	4	0	4	3	1	14
	Metzgeriaceae	1	0	0	1	1	2	2	2	2	11
	Monocleaceae	0	0	0	0	1	0	0	0	0	1
	Pallaviciniaceae	0	1	0	2	2	0	0	0	0	5
	Plagiochilaceae	2	4	4	9	10	11	17	11	10	78
	Porellaceae	0	0	0	0	1	0	0	0	0	1
	Radulaceae	0	2	0	0	4	0	1	1	2	10
	Scapaniaceae	0	0	0	0	0	1	1	1	0	3
	Trichocoleaceae	0	0	0	0	1	1	1	1	1	5
Mosses	Amblystegiaceae	0	0	0	0	0	0	0	0	1	1
	Bartramiaceae	0	0	0	0	0	0	0	1	0	1
	Bryaceae	0	0	0	0	2	1	0	1	2	6
	Calymperaceae	1	2	3	2	2	2	1	0	1	14
	Daltoniaceae	0	1	0	0	0	0	1	0	0	2
	Dicranaceae	0	0	0	3	3	4	3	3	3	19
	Hookeriaceae	0	0	0	0	1	0	0	0	0	1
	Hypnaceae	1	1	1	0	4	0	1	1	2	11
	Lembophyllaceae	0	0	0	0	0	0	1	0	0	1
	Leptodontaceae	0	1	0	0	0	0	0	0	0	1
	Meteoriaceae	1	2	0	2	4	1	3	0	2	15
	Neckeraceae	2	2	0	0	1	0	2	1	2	10
	Octoblepharaceae	1	1	1	4	0	2	1	0	0	10
	Orthotrichaceae	1	1	0	1	3	0	1	1	2	10
	Pilotrichaceae	0	1	0	0	4	0	2	1	0	8
	Plagiotheciaceae	0	0	0	0	0	0	0	0	1	1
	Pottiaceae	0	0	0	0	0	0	0	0	1	1
	Prionodontaceae	0	0	0	0	0	0	0	1	1	2
	Pterobryaceae	2	1	0	0	0	0	0	0	0	3
	Rhizogoniaceae	1	0	0	1	1	0	1	1	1	6
	Sematophyllaceae	2	2	3	3	3	1	2	1	2	19
	Stereophyllaceae	0	0	1	0	0	0	0	0	0	1
	Thuidiaceae	1	2	0	0	1	1	1	0	0	6

Table S5: Percentages of moss and liverworts species recorded across altitudinal transect

Altitude (m asl)	200	250	300	950	1500	2000	2500	3000	3600
Liverworts	61.8	65.3	70.0	76.5	74.1	84.4	80.6	83.8	69.1
Mosses	38.2	34.7	30.0	23.5	25.9	15.6	19.4	16.2	30.9

Table S6: Most abundant epiphytic bryophytes and all vascular plants recorded on three host trees

Altitude (m asl)	Epiphytic bryophytes	Vascular epiphytes
200	*Groutiella cf. tomentosa, Leptotheca, Meteorium nigrescens, Neckeropsis undulata, Plagiochila spp.*	*Orchidaceae spp, Melastomataceae sp, Araceae spp, Peperomia sp, Eugenia sp, Bromeliaceae spp, Malphigiaceae, Ephiphyllium sp,* ferns; lianas
250	*Neckeropsis undulata, Pireella cf. pohlii, Plagiochila sp, Radula sp, Zelometeorium patalum*	*Orchidaceae spp* (predominantly *Maxillaria spp*)*, Araceae spp, Piperaceae spp, Bromeliaceae sp, Cactaceae sp,* ferns; lianas
300	*Mastigiolejeunea sp, Octoblepharum albidum, Plagiochila spp, Sematophyllum subsimplex, Zelometeorium patalum*	*Orchidaceae spp, Araceae sp, Bromeliaceae spp, Rhipsalis sp, Leguminosae sp, Lentibulariaceae sp* ferns; stranglers, lianas
950	*Bazzania spp, Octoblepharum spp, Plagiochila spp*	*Orchidaceae spp, Araceae spp, Bromeliaceae spp, Peperomia sp, Melastomataceae sp, Loranthaceae sp, Ericaceae sp, Begoniaceae sp, Cyclanthaceae sp,* ferns; lianas
1500	*Bazzania spp, Bryopteris felicina, Herbertus sp, Macromitrium sp, Plagiochila spp, Stictolejeunea squamata*	*Orchidaceae spp, Araceae spp, Bromeliaceae spp, Piperaceae spp, Chusquea sp, Poaceae spp, Melastomataceae spp, Ericaceae sp, Begonia sp*, ferns; lianas
2000	*Anastrophyllum piliformis, Bazzania spp, Frullania spp, Herbertus sp, Jamesoniella rubicaulis, Lepidozia cupressina, Plagiochila spp*	*Orchidaceae spp, Bromeliaceae spp, Poaceae spp,* ferns
2500	*Anastrophyllum piliformis, Bazzania spp, Campylopus sp, Dicranum sp, Frullania spp, Herbertus spp, Jamesoniella rubicaulis, Lepicolea sp, Plagiochila spp, Scapania portoricensis*	*Orchidaceae spp, Araceae spp, Bromeliaceae spp, Melastomataceae spp, Ericaceae sp, Clusia sp*, ferns
3000	*Anastrophyllum piliformis, Bazzania spp, Campylopus sp, Dicranum sp, Frullania spp, Herbertus spp, Jamesoniella rubicaulis, Plagiochila spp, Scapania portoricensis*	*Orchidaceae spp, Bromeliaceae spp, Piperaceae sp, Chusquea sp, Poaceae spp, Melastomataceae spp, Loranthaceae sp, Viscum album, Ericaceae spp, Weinmannia sp, Clusia sp,* ferns

3600	*Campylopus sp, Dicranum sp, Frullania spp, Herbertus spp, Plagiochila spp, Prionodon cf. fuscolutescens*	*Orchidaceae spp, Bromeliaceae spp, Ericaceae sp, Asteraceae sp, Oxalis sp, Piperaceae spp, Ericaceae sp,* ferns

28

29

30 **Fig S1**. Non-linear regression function ("Tree A-dbh model"), based on allometric calculations and
31 existing plot census data (dbh for all trees >10 cm) used to estimate total surface area in one hectare
32 plot: $y = 7.96e^{0.029x}$

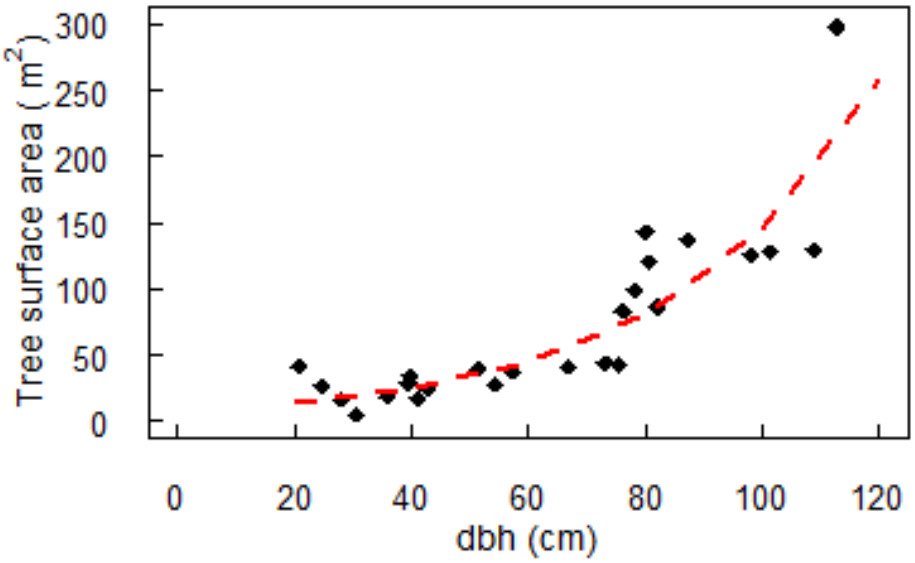

47

48

49

50

Supplementary Information Continued: Data used for Figures

Figure 2 a and c								
Altitude (m asl)	**$\delta^{13}C$ (‰)**	**C:N**	**Altitude (m asl)**	**$\delta^{13}C$ (‰)**	**C:N**	**Altitude (m asl)**	**$\delta^{13}C$ (‰)**	**C:N**
200	-32.39	32.1	1500	-26.94	41.6	3000	-27.43	89.3
200	-31.64	34.2	1500	-31.34	43.6	3000	-23.75	91.1
200	-33.51	25.6	1500	-29.17	50	3000	-27.17	61.8
200	-30.53	40.3	1500	-29.98	45.8	3000	-29.43	65.2
200	-33.89	23.6	1500	-29.24	63.7	3000	-27.05	88.4
200	-31.93	33	1500	-32.5	23.1	3000	-26.32	92.6
200	-34.95	22.7	1500	-32.38	43	3000	-29.7	59
200	-35.27	23.3	1500	-34.57	25	3000	-25.22	79.5
200	-29.67	24	1500	-27.55	49.6	3000	-29.21	65
200	-30.29	29.3	1500	-27.51	50.1	3000	-27.6	69.2
200	-34.68	32.5	1500	-30.94	75.9	3000	-28.07	74.5
200	-33.64	36.1	1500	-29.18	73.8	3000	-29.26	74.4
250	-30.83	27	1500	-30.7	66.1	3000	-28.63	123.1
250	-31.14	32.4	1500	-28.63	34.7	3000	-29.75	64.8
250	-31.43	32.6	1500	-29.91	37.1	3000	-30.43	80.4
250	-31.05	31.8	1500	-30.3	42.3	3000	-27.55	94.5
250	-31.02	34.8	1500	-28.77	42.1	3000	-24.43	81.2
250	-31.49	30.7	1500	-28.45	66.6	3000	-26.52	79.8
250	-33.91	27	1500	-29.72	39.6	3000	-27.3	78.4
250	-31.25	26.6	1500	-29.19	34.8	3000	-24.8	93.9
250	-32.06	22.6	1500	-30.52	62.6	3000	-25.5	95
250	-31.69	19.7	1500	-30.01	47.6	3000	-25.67	68.6
250	-33.01	18.3	1500	-30.83	71.5	3000	-24.92	90.4
250	-35.11	23.3	1500	-30.84	NA	3000	-28.07	59.3
250	-35.22	20.7	2000	-28.21	74.4	3600	-26.3	68.9
250	-34.71	20.8	2000	-27.32	69	3600	-26.67	55.7
250	-35.31	21.1	2000	-27.78	78.3	3600	-29.43	45.1
250	-31.78	41.3	2000	-28.96	66.9	3600	-28.85	36.9
250	-32.85	31.8	2000	-28.6	45	3600	-29	60.5
250	-33.91	46.1	2000	-27.76	63.5	3600	-27.99	51.6
300	-29.49	31.8	2000	-29.02	75.8	3600	-27.29	37
300	-30.56	19.6	2000	-30.15	49	3600	-29.78	36.6
300	-28.88	26.8	2000	-27.24	77.2	3600	-25.34	95.4
300	-32.27	20.2	2000	-26.44	63.4	3600	-27.24	70.8
300	-35.89	21.3	2000	-27.51	61.9	3600	-27.74	87.6
300	-29.58	28.5	2000	-29.99	72.6	3600	-28.98	100.8
300	-31.39	20	2000	-28.54	56.8	3600	-27.6	28.3
300	-31.84	19.7	2000	-29.8	55.5	3600	-27.24	53

300	-34.96	31.6		2000	-28.86	47.6		3600	-33.28	39.3
300	-35.89	24.2		2000	-29.27	45.4		3600	-31.11	47.6
300	-30.66	38.1		2000	-28.29	64.4		3600	-26.85	42.4
300	-31.97	22.4		2000	-28.65	43.1		3600	-29.7	30.4
300	-31.31	33.7		2000	-26.8	65.1		3600	-26.79	61
300	-30.43	27		2000	-27.6	82.1		3600	-27.05	65.8
300	-34.09	30.6		2000	-27.53	85.1		3600	-33.08	30.4
1000	-28.34	62.3		2000	-28.09	96		3600	-32.15	66.8
1000	-30.99	27.7		2000	-30.56	76.8		3600	-31.04	48.6
1000	-29.31	39.6		2000	-28.98	82.8		3600	-28.25	43.6
1000	-29.19	42.4		2500	-25.52	74.4				
1000	-29.53	46.5		2500	-27.03	102.5				
1000	-30.83	58.4		2500	-26.37	93.5				
1000	-33.05	26.7		2500	-25.94	114.3				
1000	-29.73	39.5		2500	-27.78	87.1				
1000	-29.37	65.6		2500	-27.1	87.4				
1000	-28.56	59.4		2500	-30.06	49.1				
1000	-30.43	53		2500	-30.22	61.2				
1000	-30.32	43.4		2500	-27.2	77.3				
1000	-31.92	38.1		2500	-25.82	89.9				
1000	-29.24	43		2500	-26.37	82				
1000	-29.88	56.8		2500	-26.08	85.6				
1000	-30.67	57.9		2500	-26.42	78.6				
1000	-26.47	59.5		2500	-27.39	82.7				
1000	-28.63	68.4		2500	-28.36	69.3				
1000	-28.48	30.3		2500	-27.31	65.3				
1000	-31.51	48.6		2500	-27.52	74.9				
1000	-32.79	43.7		2500	-26.82	80.2				
1000	-31.59	23		2500	-28.4	84.8				
1000	-33.39	24.4		2500	-25.72	106.2				
1000	-33.13	NA		2500	-28.74	84.3				
				2500	-27.17	94.5				
				2500	-29.15	55.6				
				2500	-27.75	82.7				

53

54

Figure 2b									
MAVPD (kPa)	$\delta^{13}C$ (‰)		MAVPD (kPa)	$\delta^{13}C$ (‰)		MAVPD (kPa)	$\delta^{13}C$ (‰)		MAVPD (kPa)	$\delta^{13}C$ (‰)
0	-28.21		0.01	-27.52		0.04	-25.34		0.28	-28.34
0	-27.32		0.01	-26.82		0.04	-27.24		0.28	-30.99
0	-27.78		0.01	-28.4		0.04	-27.74		0.28	-29.31
0	-28.96		0.01	-25.72		0.04	-28.98		0.28	-29.19
0	-28.6		0.01	-28.74		0.04	-27.6		0.28	-29.53
0	-27.76		0.01	-27.17		0.04	-27.24		0.28	-30.83
0	-29.02		0.01	-27.75		0.04	-33.28		0.28	-33.05
0	-30.15		0.01	-29.15		0.04	-31.11		0.28	-29.73
0	-27.24		0.02	-27.43		0.04	-26.85		0.28	-29.37
0	-26.44		0.02	-23.75		0.04	-29.7		0.28	-28.56
0	-27.51		0.02	-27.17		0.04	-26.79		0.28	-30.43
0	-29.99		0.02	-29.43		0.04	-27.05		0.28	-30.32
0	-28.54		0.02	-27.05		0.04	-33.08		0.28	-31.92
0	-29.8		0.02	-26.32		0.04	-32.15		0.28	-29.24
0	-28.86		0.02	-29.7		0.04	-31.04		0.28	-29.88
0	-29.27		0.02	-25.22		0.04	-28.25		0.28	-30.67
0	-28.29		0.02	-29.21		0.19	-26.94		0.28	-26.47
0	-28.65		0.02	-27.6		0.19	-31.34		0.28	-28.63
0	-26.8		0.02	-28.07		0.19	-29.17		0.28	-28.48
0	-27.6		0.02	-29.26		0.19	-29.98		0.28	-31.51
0	-27.53		0.02	-28.63		0.19	-29.24		0.28	-32.79
0	-28.09		0.02	-29.75		0.19	-32.5		0.28	-31.59
0	-30.56		0.02	-30.43		0.19	-32.38		0.28	-33.39
0	-28.98		0.02	-27.55		0.19	-34.57		0.28	-33.13
0.01	-25.52		0.02	-24.43		0.19	-27.55		0.34	-30.83
0.01	-27.03		0.02	-26.52		0.19	-27.51		0.34	-31.14
0.01	-26.37		0.02	-27.3		0.19	-30.94		0.34	-31.43
0.01	-25.94		0.02	-24.8		0.19	-29.18		0.34	-31.05
0.01	-27.78		0.02	-25.5		0.19	-30.7		0.34	-31.02
0.01	-27.1		0.02	-25.67		0.19	-28.63		0.34	-31.49
0.01	-30.06		0.02	-24.92		0.19	-29.91		0.34	-33.91
0.01	-30.22		0.02	-28.07		0.19	-30.3		0.34	-31.25
0.01	-27.2		0.04	-26.3		0.19	-28.77		0.34	-32.06
0.01	-25.82		0.04	-26.67		0.19	-28.45		0.34	-31.69
0.01	-26.37		0.04	-29.43		0.19	-29.72		0.34	-33.01
0.01	-26.08		0.04	-28.85		0.19	-29.19		0.34	-35.11
0.01	-26.42		0.04	-29		0.19	-30.52		0.34	-35.22
0.01	-27.39		0.04	-27.99		0.19	-30.01		0.34	-34.71
0.01	-28.36		0.04	-27.29		0.19	-30.83		0.34	-35.31
0.01	-27.31		0.04	-29.78		0.19	-30.84		0.34	-31.78
									0.34	-32.85
									0.34	-33.91

Figure 2d							
MAVPD (kPa)	$\delta^{18}O$ (‰)	MAVPD (kPa)	$\delta^{18}O$ (‰)	MAVPD (kPa)	$\delta^{18}O$ (‰)	MAVPD (kPa)	$\delta^{18}O$ (‰)
0	15.95	0.02	16.4	0.19	16.53	0.34	17.9
0	16.79	0.02	15.08	0.19	15.38	0.34	18.8
0	15.77	0.02	14.69	0.19	16.68	0.34	18.3
0	16.66	0.02	16.03	0.19	17.63	0.34	17.7
0	16.94	0.02	15.59	0.19	15.96	0.34	17.8
0	15.72	0.02	16.69	0.19	15.81	0.34	17.2
0	15.73	0.02	16.9	0.19	16.61	0.34	18.3
0	15.58	0.02	16.87	0.19	16.25	0.34	20.1
0	14.89	0.02	16.57	0.19	16.02	0.34	17.3
0	15.18	0.02	15.97	0.19	15.57	0.34	17.3
0	16.22	0.02	17.91	0.19	16.44	0.34	18.8
0	17.27	0.02	16.53	0.19	17.35	0.34	17.2
0	16.67	0.02	17.01	0.19	17.48	0.34	16.7
0	16.24	0.02	18.04	0.19	17.04	0.34	17.1
0	17.03	0.02	18.09	0.19	16.78	0.34	17.2
0	16.35	0.02	17.1	0.19	16.92	0.34	18
0	16.97	0.02	17.13	0.19	16.01	0.34	17.7
0	17.77	0.02	16.47	0.19	16.51	0.34	18.5
0	18.63	0.02	15.87	0.19	16.55	0.34	17.4
0	16.91	0.02	17.09	0.19	17.87	0.34	19.5
0	19.04	0.02	16.61	0.19	17.82	0.34	17.5
0	18.25	0.02	16.95	0.19	19.04	0.34	17.7
0	17.92	0.02	17.14	0.19	19.54	0.34	19.6
0	18.48	0.02	16.48	0.19	16.95	0.34	18.8
0.01	16.46	0.04	17.46	0.28	17.24	0.34	18.7
0.01	16.13	0.04	16.53	0.28	16.01	0.34	19.3
0.01	15.51	0.04	16.6	0.28	16.52	0.34	19.1
0.01	16.93	0.04	16.3	0.28	17.84	0.34	18.5
0.01	19.13	0.04	18.71	0.28	17.91	0.34	17
0.01	16.65	0.04	16.16	0.28	16.93	0.34	18.6
0.01	15.14	0.04	15.85	0.28	17.49	0.34	17.5
0.01	17.32	0.04	16.22	0.28	16.59	0.34	17.4
0.01	15.5	0.04	15.82	0.28	17.74	0.34	18.3
0.01	15.89	0.04	15.13	0.28	17.79	0.34	17.6
0.01	17.41	0.04	15.4	0.28	18.75	0.34	16.9
0.01	17.12	0.04	16.22	0.28	17.09	0.34	18.3
0.01	16.76	0.04	15.6	0.28	17.12	0.34	16.4
0.01	16.71	0.04	15.37	0.28	19.03	0.34	17
0.01	15.64	0.04	16.08	0.28	17.15	0.34	17.7
0.01	16.88	0.04	16.65	0.28	17.38	0.34	16.2
0.01	15.85	0.04	15.66	0.28	17.49	0.34	19.8
0.01	16.01	0.04	16.85	0.28	17.76	0.34	18.3
0.01	17.05	0.04	16.58	0.28	17.24	0.34	20.4
0.01	17.09	0.04	16.08	0.28	19.14	0.34	20.4
0.01	16.22	0.04	16.68	0.28	18.13	0.34	20
0.01	17.87	0.04	15.49	0.28	18.49		
0.01	18.63	0.04	17.49	0.28	18.43		
0.01	16.76	0.04	15.74	0.28	18.52		

Figure 3a				Figure 3b		
Altitude (m asl)	**Liverwort Species**	**Moss Species**	**Total Species**	**Moss species m^{-2}**	**Liverwort species m^{-2}**	**Total species m^{-2}**
200	21	13	34	0.0068	0.0386	0.0832
250	32	17	49	0.0388	0.0706	0.1088
300	21	9	30	0.0198	0.058	0.0962
950	52	16	68	0.0784	0.2568	0.346
1500	83	29	112	0.1242	0.379	0.4936
2000	65	12	77	0.24	1.501	1.8068
2500	83	20	103	0.292	0.8716	1.0818
3000	62	12	74	0.2292	1.1402	1.363
3600	47	21	68	0.1668	0.377	0.5554

78

Figure 4 a-d								
	Humus (kg m^{-2})							
Altitude (m asl)	**Upper Canopy**	**SE**	**Mid-canopy**	**SE**	**Lower Canopy**	**SE**	**Head Height**	**SE**
250	0.07	0.04	0.04	0.02	0.04	0.02	0.00	0.00
950	0.13	0.06	0.52	0.18	0.84	0.59	0.13	0.05
1500	0.06	0.02	0.06	0.02	0.05	0.01	0.05	0.02
2000	0.57	0.18	1.57	0.44	0.77	0.22	0.36	0.12
2500	0.66	0.29	0.99	0.24	2.60	0.68	0.66	0.36
3000	0.59	0.14	2.30	1.20	2.19	1.01	0.83	0.32
3600	1.14	0.38	1.44	0.41	2.81	1.01	1.48	0.93
	Bryophytes (kg m^{-2})							
Altitude (m asl)	**Upper Canopy**	**SE**	**Mid-canopy**	**SE**	**Lower Canopy**	**SE**	**Head Height**	**SE**
250	0.01	0.01	0.05	0.03	0.02	0.01	0.01	0.00
950	0.12	0.05	0.13	0.07	0.09	0.02	0.03	0.01
1500	0.12	0.04	0.08	0.02	0.09	0.03	0.04	0.02
2000	0.22	0.04	0.50	0.27	0.22	0.09	0.12	0.04
2500	0.71	0.15	1.06	0.49	0.36	0.08	0.18	0.05
3000	1.62	1.22	1.40	0.54	0.76	0.19	0.26	0.07
3600	0.59	0.08	0.97	0.51	0.26	0.06	1.10	0.86
	Vascular epiphytes (kg m^{-2})							
Altitude (m asl)	**Upper Canopy**	**SE**	**Mid-canopy**	**SE**	**Lower Canopy**	**SE**	**Head Height**	**SE**
250	0.09	0.03	0.08	0.03	0.11	0.05	0.01	0.00
950	0.10	0.05	0.36	0.06	0.28	0.06	0.15	0.09
1500	0.09	0.02	0.20	0.13	0.15	0.10	0.04	0.04
2000	1.37	0.55	1.15	0.67	0.97	0.49	0.41	0.20
2500	1.06	0.38	0.86	0.23	1.42	0.52	0.39	0.31
3000	0.92	0.53	1.06	0.37	0.95	0.61	0.31	0.21
3600	0.14	0.09	0.03	0.02	0.12	0.06	0.63	0.45

79

80

81

82

Figure 5a: Epiphyte Cover								
Altitude (m asl)	**Cover Type**	**Cover (%)**	**SE (%)**		**Altitude (m asl)**	**Cover Type**	**Cover (%)**	**SE (%)**
250	Bryophyte	10.4	13.1		2000	Bryophyte	57.7	18.5
250	Vascular	9.6	3.5		2000	Vascular	25.2	5.3
250	Lichen	35.1	6.2		2000	Lichen	4.9	0.6
250	Bare	47.0	6.3		2000	Bare	24.1	13.8
950	Bryophyte	34.8	5.9		2500	Bryophyte	61.2	10.1
950	Vascular	23.2	8.5		2500	Vascular	31.0	12.6
950	Lichen	10.1	4.1		2500	Lichen	3.5	1.5
950	Bare	40.0	11.5		2500	Bare	26.1	12.3
1500	Bryophyte	36.5	10.9		3000	Bryophyte	80.9	6.1
1500	Vascular	11.6	3.8		3000	Vascular	34.8	22.2
1500	Lichen	6.7	1.5		3000	Lichen	3.5	1.8
1500	Bare	39.1	12.1		3000	Bare	6.1	5.8
					3600	Bryophyte	70.7	4.9
					3600	Vascular	7.2	2.6
					3600	Lichen	9.3	5.6
					3600	Bare	10.4	3.8

83

Figure 5b: Biomass						
Altitude (m asl)	**Humus (t ha^{-1})**	**Humus SE (t ha^{-1})**	**Bryophytes (t ha^{-1})**	**Bryophyte SE (t ha^{-1})**	**Vascular Epiphytes (t ha^{-1})**	**Vascular Epiphytes SE (t ha^{-1})**
250	0.4	0.2	0.2	0	0.8	0.2
950	3.8	1.4	0.8	0.2	2	0.4
1500	0.8	0.2	1.4	0.2	2	0.6
2000	10.6	2	3.4	1	12.6	3.2
2500	20.2	4.2	9.6	2.4	15.4	3.2
3000	13.2	3.6	9	3	7.2	2
3600	18	4	7.6	2.6	2.4	1.2

84

Figure 5c: Water retention capacity						
Altitude (m asl)	**Humus (mm)**	**Humus SE (mm)**	**Bryophytes (mm)**	**Bryophyte SE (mm)**	**Vascular Epiphytes (mm)**	**Vascular Epiphytes SE (mm)**
250	0.16	0.05	0.16	0.16	0.32	0.05
950	1.73	0.81	0.86	0.27	0.65	0.16
1500	0.65	0.11	1.57	0.32	0.59	0.32
2000	5.51	1.24	2.70	0.38	3.51	1.03
2500	9.84	2.00	7.46	2.70	4.00	1.14
3000	7.24	2.32	6.38	2.38	3.30	1.24
3600	8.05	2.32	4.81	2.05	0.49	0.43

85

86